A Mechanistic Investigation of the Polymerization of Ethylene Catalyzed by Neutral Ni(II) Complexes Derived from Bulky Anilinotropone Ligands

Jason C. Jenkins and Maurice Brookhart*

Contribution from the Department of Chemistry, University of North Carolina at Chapel Hill, Chapel Hill, North Carolina 27599

Received November 21, 2003; E-mail: mbrookhart@unc.edu

Abstract: An extensive mechanistic investigation has been carried out on ethylene polymerizations catalyzed by neutral Ni(II) catalysts derived from bulky anilinotropone ligands. Complexes and precatalysts prepared include aryl derivatives [(2,6-i-Pr$_2$C$_6$H$_3$)NC$_7$H$_4$O(7-Aryl)Ni(Ph)(PPh$_3$)] (**9**, Aryl = phenyl(**a**), 1-naphthyl(**b**), p-methoxyphenyl(**c**), p-trifluoromethylphenyl(**d**)), alkyl derivatives [[(2,6-^{i}Pr$_2$C$_6$H$_3$)NC$_7$H$_5$O]Ni(R)(2,4-lutidine)] (**16**, R = Et (**a**), n-Pr (**b**)) and [[(2,6-^{i}Pr$_2$C$_6$H$_3$)NC$_7$H$_5$O]Ni(R)(PPh$_3$)] (**17**, R = Et (**a**), n-Pr (**b**), n-hexyl (**c**), i-Pr (**d**)), and the nickel hydride complex [[(2,6-^{i}Pr$_2$C$_6$H$_3$)NC$_7$H$_5$O]Ni(H)(PPh$_3$)], **20**. Branched polyethylenes are produced at 40–80 °C in toluene with M_n values in the 100–200K range and molecular weight distributions of ca. 1.4–2.2. Branching ranges from 15 to 64 branches/1000 carbons depending on temperature and ethylene pressure. The electron-withdrawing −CF$_3$ substituent on the 7-aryl group increases activity but has little effect on branching and molecular weight. NMR experiments establish that in the case of the PPh$_3$-substituted systems, the catalyst rests as an equilibrating mixture of the alkyl phosphine and the alkyl ethylene complexes. At high ethylene pressures, the turnover frequency saturates, indicating that the equilibrium has shifted nearly completely to the alkyl olefin complex. Under these conditions, the barriers to migratory insertion were determined to be ca. 16–17 kcal/mol for **9a**, **9c**, **9d**, and **16a**. Extraction of 2,6-lutidine from complexes **16a,b** yields highly dynamic β-agostic alkyl complexes [[(2,6-i-Pr$_2$C$_6$H$_3$)NC$_7$H$_5$O]-Ni(Et)] **21** and [[(2,6-i-Pr$_2$C$_6$H$_3$)NC$_7$H$_5$O]Ni(i-Pr)] **22**. Free energy barriers to nickel−carbon bond rotation and β-hydride elimination of 11.1 and ca. 17 kcal/mol, respectively, were determined for **22**. Themolysis of **17c** at 50 °C generates hydride **20** and hexene and occurs by two pathways, one independent of [PPh$_3$] and one retarded by PPh$_3$. At much slower rates, hydride **20** reductively eliminates free ligand, which ultimately generates a bis-ligand complex, **25**. Catalyst decay under polymerization conditions was shown to occur by a similar process to generate free ligand and a bis-ligand complex formed by reaction of free ligand with an active catalyst species. The major chain transfer route is a simple β-elimination process, not chain transfer to monomer.

Introduction

Interest in late transition metal olefin polymerization catalysts has mushroomed over the past decade.[1–4] Work in the 1980s showed that Ni(II) complexes containing modified SHOP ligands catalyzed ethylene polymerization, but in general, such systems exhibited modest activities and lifetimes and broad molecular weight distributions.[5–9] A major advance in the area of late metal catalysis came with the discovery of Ni(II) and Pd(II) catalysts derived from bulky aryl-substituted α-diimines of general structure **1**.[10–16]

M = Ni, **1a**
Pd, **1b**
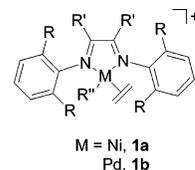
These systems are not only highly effective ethylene polymerization catalysts but also convert α-olefins, trans-1,2-disubstituted olefins, and certain cyclic olefins to high-molar mass materials.[2,10–15,17] The microstructures of the polymers obtained are quite different than those observed for polymers prepared

(1) Boffa, L. S.; Novak, B. M. *Chem. Rev.* **2000**, *100*, 1479.
(2) Ittel, S. D.; Johnson, L. K.; Brookhart, M. *Chem. Rev.* **2000**, *100*, 1169.
(3) Britovsek, G. J. P.; Gibson, V. C.; Wass, D. F. *Angew. Chem., Int. Ed.* **1999**, *38*, 428.
(4) Mecking, S. *Coord. Chem. Rev.* **2000**, *203*, 325.
(5) Keim, W.; Hoffman, B.; Lodewick, R.; Peiukert, M.; Schmitt, G. *J. Mol. Catal.* **1979**, *6*, 79.
(6) Keim, W. *Angew. Chem., Int. Ed. Engl.* **1990**, *29*, 235.
(7) Peuckert, M.; Keim, W. *Organometallics* **1983**, *2*, 594.
(8) Ostoya Starzewski, K. A.; Witte, J. *Angew. Chem., Int. Ed. Engl.* **1985**, *24*, 599.
(9) Klabunde, U.; Ittel, S. D. *J. Mol. Catal.* **1987**, *41*, 123.

(10) Johnson, L. K.; Killian, C. M.; Brookhart, M. *J. Am. Chem. Soc.* **1995**, *117*, 6414.
(11) Killian, C. M.; Tempel, D. J.; Johnson, L. K.; Brookhart, M. *J. Am. Chem. Soc.* **1996**, *118*, 11664.
(12) Gates, D. P.; Svejda, S. A.; Onate, E.; Killian, C. M.; Johnson, L. K.; White, P. S.; Brookhart, M. *Macromolecules* **2000**, *33*, 2320.
(13) Johnson, L. K.; Mecking, S.; Brookhart, M. *J. Am. Chem. Soc.* **1996**, *118*, 267.
(14) Mecking, S.; Johnson, L. K.; Wang, L.; Brookhart, M. *J. Am. Chem. Soc.* **1998**, *120*, 888.
(15) Leatherman, M. D.; Brookhart, M. *Macromolecules* **2001**, *34*, 2748.

from early metal catalysts. For example, the polyethylenes produced range from linear to highly branched to hyperbranched depending on metal, ligand structure, ethylene pressure, and temperature.[10,12,18,19] Poly(α-olefin)s made from diimine catalysts contain fewer branches than expected and are termed "chain-straightened".[2,11]

Extensive mechanistic[20–24] and theoretical[25–27] investigations of the diimine catalysts have been reported. The key to forming a high polymer is the presence of substituents at the ortho positions of the aryl rings, which places bulk in the axial sites of the square planar complexes and retards chain transfer. The unusual branching features observed are a result of migration of the metal along the polymer chain via β-elimination/readdition ("chain walking") prior to insertion. The dynamics of these processes, the nature of the catalyst resting states, the barriers to olefin insertions, and other mechanistic details have been elucidated for a series of diimine Ni and Pd catalysts.[22–24]

In contrast to early metal catalysts, the late metal systems are much less oxophilic and therefore potentially more compatible with monomers bearing functional groups. This feature has attracted considerable interest in that the ability to copolymerize ethylene with functionalized monomers, especially readily available vinyl monomers, would allow access to a wide range of new, inexpensive ethylene copolymers. Limited success has been achieved in this regard.[28] For example, Pd(II) diimine catalysts were shown to copolymerize ethylene and methyl acrylate, but formation of a chelate complex involving the carbonyl group greatly reduces the turnover frequency.[14] More recently, the Ni(II) diimine complexes were also shown to effect this copolymerization but only at high temperatures, and again turnover frequencies were low.[29] Monomers possessing more remote functional groups inaccessible to the metal via chain walking are viable, while other monomers poison the diimine systems.[2,30,31]

In that the electrophilic nature of the cationic Ni and Pd complexes still presents problems with respect to incorporation

of polar monomers, renewed interest arose in developing neutral (less electrophilic) nickel systems for use with polar monomers and polar solvents. As a major design feature, most second-generation neutral Ni catalysts have incorporated a bulky ortho-substituted aryl imine moiety in analogy with catalysts **1a,b**. Groups from DuPont and Caltech have reported a family of neutral nickel ethylene polymerization catalysts based on the deprotonated salicylaldimine ligand in which the imine substituent is a bulky ortho-disubstituted aryl group.[30–33] The DuPont group has reported use of allyl complexes, **2a**, as initiators where the most active catalysts bear nitro substituents on the aryl ring, whereas the Caltech group uses the phosphine complexes, **2b,c** as initiators. Catalyst **2c**, bearing a bulky 9-anthracenyl substituent was found to be particularly productive and has been used to copolymerize ethylene and functionalized norbornenes.[31]
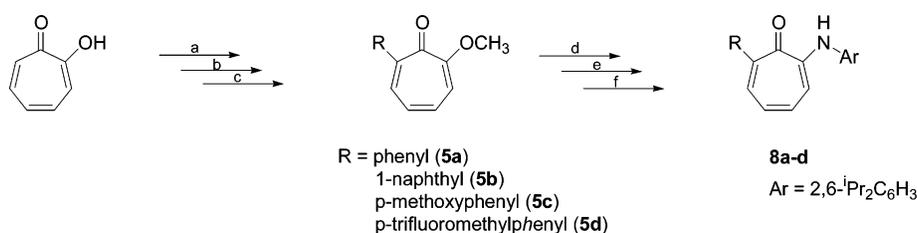

2a
G = Functional group(s)

R = H, **2b**
R = 9-anthracenyl, **2c**
Ar = 2,6-^{i}Pr$_2$C$_6$H$_3$
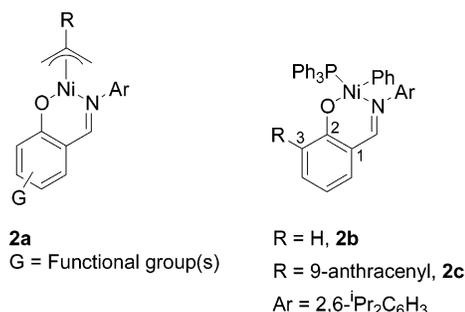
Recently, we have reported neutral nickel catalysts based on both 2-anilinotropone, **3**,[34] and 2-anilinoperinaphthenone, **4**.[35] High initial turnover frequencies were observed with these catalysts and substitution of the tropone backbone at the 7-position with bulky aryl substituents resulted in increased polyethylene productivity at low temperatures. In addition, the effects of substitution of the *N*-aryl ring with a variety of alkyl and aryl groups and halides has been reported.[36]

3

4
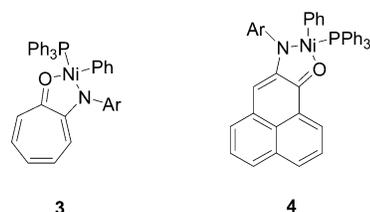
In contrast to the cationic diimine-based nickel catalysts, there is relatively little mechanistic information available for these or any neutral nickel ethylene polymerization systems. In light of the increasing interest in the neutral systems, it was the goal of this work to develop a full mechanistic picture of a typical neutral catalyst system. We report here in-depth studies of ethylene polymerizations catalyzed by the anilinotropone complexes, **3**. Detailed information concerning the chain propagation process, the barrier to ethylene insertion, the nature and

(16) Brookhart, M. S.; Johnson, L. K.; Killian, C. M.; Arthur, S. D.; Feldman, J.; McCord, E. F.; McLain, S. J.; Kreutzer, K. A.; Nennet, A. M. A.; Coughlin, E. B.; Ittel, S. D.; Parthasarathy, A.; Tempel, D. J. WO Patent Application 9623010 to DuPont, 1995.
(17) McLain, S. J.; Feldman, J.; McCord, E. F.; Garner, K. H.; Teasley, M. F.; Coughlin, E. B.; Sweetman, K. J.; Johnson, L. K.; Brookhart, M. *Macromolecules* **1998**, *31*, 6705.
(18) Cotts, P. M.; Guan, Z.; McCord, E.; McLain, S. *Macromolecules* **2000**, *33*, 6945.
(19) Guan, Z.; Cotts, P. M.; McCord, E. F.; McLain, S. J. *Science* **1999**, *283*, 2059.
(20) Tempel, D. J.; Brookhart, M. *Organometallics* **1998**, *17*, 2290.
(21) Svejda, S. A.; Johnson, L. K.; Brookhart, M. *J. Am. Chem. Soc.* **1999**, *121*, 10634.
(22) Tempel, D. J.; Johnson, L. K.; Huff, R. L.; White, P. S.; Brookhart, M. *J. Am. Chem. Soc.* **2000**, *122*, 6686.
(23) Shultz, L. H.; Tempel, D. J.; Brookhart. M. *J. Am. Chem. Soc.* **2001**, *123*, 11539.
(24) Leatherman, M. D.; Svejda, S. A.; Johnson, L. K.; Brookhart, M. *J. Am. Chem. Soc.* **2003**, *125*, 3068.
(25) Chan, M. S. W.; Deng, L.; Ziegler, T. *Organometallics* **2000**, *19*, 2741.
(26) Deng, L.; Margl, P.; Ziegler, T. *J. Am. Chem. Soc.* **1997**, *119*, 1094.
(27) Deng, L.; Woo, T. K.; Cavallo, L.; Margl, P. M.; Ziegler, T. *J. Am. Chem. Soc.* **1997**, *119*, 6177.
(28) Ethylene has been successfully copolymerized with vinyl silanes using both nickel and palladium diimine catalysts: Johnson, L. K.; McLain, S. J.; Sweetman, K. J.; Wang, Y.; Bennett, A. M. A.; Wang, L.; McCord, E. F.; Ionkin, A.; Ittel, S. D.; Radzewich, C. E.; Schiffino, R. S. WO200344066, 2003.
(29) Johnson, L.; Bennett, A.; Dobbs, K.; Hauptman, E.; Ionkin, A.; Ittel, S.; McCord, E.; McLain, S.; Radzewich, C.; Yin, Z.; Wang, L.; Wang, Y.; Brookhart, M. *Polym. Mater. Sci. Eng.* **2002**, *86*, 319.
(30) Wang, C.; Friedrich, S.; Younkin, T. R.; Li, R. T.; Grubbs, R. H.; Bansleben, D. A.; Day, M. W. *Organometallics* **1998**, *17*, 3149.
(31) Younkin, T. R.; Connor, E. F.; Henderson, J. I.; Friedrich, S. K.; Grubbs, R. H.; Bansleben, D. A. *Science* **2000**, *287*, 460.

(32) Johnson, L. K.; Bennett, A. M. A.; Ittel, S. D.; Wang, L.; Parthasarathy, A.; Hauptman, E.; Simpson, R. D.; Feldman, J.; Coughlin, E. B. WO 98/30609, 1998.
(33) Connor, E. F.; Younkin, T. R.; Henderson, J. I.; Waltman, A. W.; Grubbs, R. H. *Chem. Commun.* **2003**, 2272.
(34) Hicks, F. A.; Brookhart, M. *Organometallics* **2001**, *20*, 3217.
(35) Jenkins, J. C.; Brookhart, M. *Organometallics* **2003**, *22*, 250.
(36) Hicks, F. A.; Jenkins, J. C.; Brookhart, M. *Organometallics* **2003**, *22*, 3533.

Scheme 1 [a]

R = phenyl (**5a**)
1-naphthyl (**5b**)
p-methoxyphenyl (**5c**)
p-trifluoromethyl*p*henyl (**5d**)

8a-d

Ar = 2,6-^{i}Pr$_2$C$_6$H$_3$

[a] Reaction conditions: (a) ^{n}Bu$_4$NOH, CH$_3$I; (b) NBS; (c) ArB(OH)$_2$, Pd(PPh$_3$)$_4$; (d) HCl/MeOH; (e) Tf$_2$O, pyridine; (f) H$_2$NAr, Pd$_2$dba$_3$, BINAP.

Scheme 2

**10** **11** **12**

13
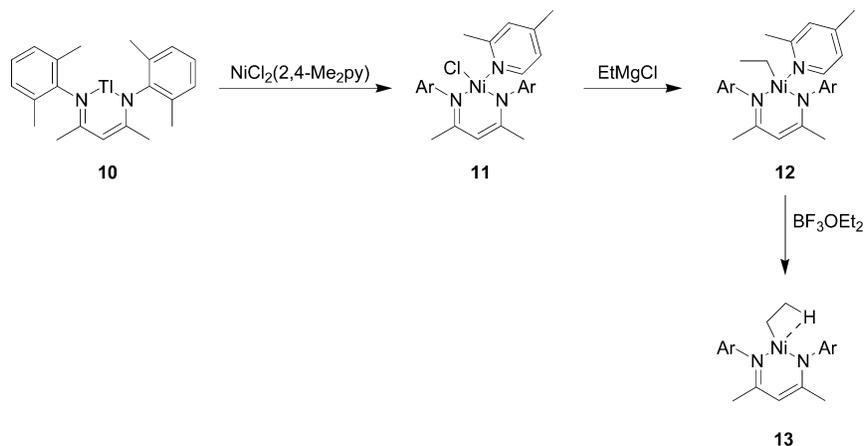
dynamics of the intermediate Ni alkyl complexes, and the chain transfer and catalyst decay processes are reported.

Results and Discussion

Syntheses of Catalysts and Intermediates. 2-Anilino-7-aryltropone Nickel(II)(phenyl)(PPh$_3$) Complexes. Procedures for the preparation of 2-(2,6-diisopropyl)anilino-7-phenyltropone (**8a**) and 2-(2,6-diisopropylanilino-7-(1-naphthyl)tropone (**8b**) ligands and their corresponding neutral nickel(II) catalysts, **9a** and **9b**, have been reported.[36] To investigate electronic effects in these catalyst systems 2-(2,6-diisopropyl)anilino-7-(*p*-methoxyphenyl)tropone (**8c**) and 2-(2,6-diisopropyl)anilino-7-(*p*-trifluoromethylphenyl)tropone (**8d**) were synthesized using procedures reported for the general preparation of 2-anilino-7-aryltropone ligands (Scheme 1). Tropolone was converted to methoxytropone[37] and brominated with *N*-bromosuccinimide to produce 2-methoxy-7-bromotropone.[38] Either (*p*-methoxyphenyl)boronic acid or (*p*-trifluoromethylphenyl)boronic acid were coupled with 2-methoxy-7-bromotropone to yield 2-methoxy-7-aryltropones **8c** and **8d**, respectively.[39] Demethylation,[39] conversion to the triflate with triflic anhydride,[40] and coupling with 2,6-diisopropylaniline under typical Buchwald−Hartwig coupling conditions produced the 2-anilino-7-aryltropones **8c,d**.[36] The overall conversion proceeded in significantly better yields for the methoxy-substituted ligand than the trifluoromethyl-substituted ligand. The increased solubility of the trifluoro-methyl-substituted intermediates led to lower yields in steps that required recrystallization. Ligands **8c,d** were characterized by ^{1}H, ^{13}C, and, for **8d**, ^{19}F NMR spectroscopy. The spectra differ little from those reported for 2-anilino-7-phenyltropone, **8a**[36] (see Experimental Section).

Ligands **8c,d** were converted to the (2-anilino-7-aryltropone)-nickel(II) complexes **9c,d** using the procedure reported for the preparation of (2-anilino-7-phenyltropone)nickel(PPh$_3$)(Ph) (eq 1).[36] The ligands were deprotonated in THF with NaH, and solid (PPh$_3$)$_2$Ni(Ph)(Cl) was added and the reaction mixture stirred for 1 h. Following filtration and recrystallization, complexes **9c,d** were obtained in 63 and 29% yields, respectively. Complexes **9c,d** were characterized by ^{1}H, ^{13}C, ^{31}P, and ^{19}F NMR (**9d**). Two distinct doublets at 1.2 and 1.0 ppm were observed in the ^{1}H NMR spectrum for both **9c,d**, indicating restricted rotation about the N−aryl bond, which renders each methyl group of an isopropyl unit inequivalent. Additional NMR data for **9c,d** are summarized in the Experimental Section.

8a-d

Ar = 2,6-^{i}Pr$_2$C$_6$H$_3$

9a-d

(1)
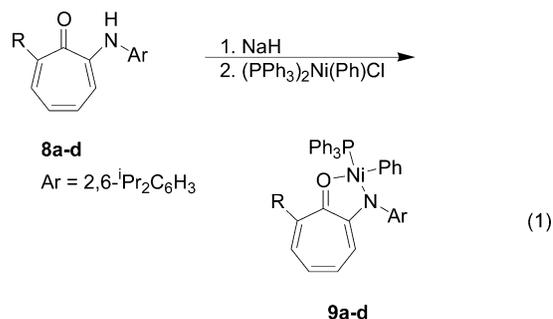
(2-Anilinotropone)Ni(II)(alkyl)(L) (L = 2,4 Lutidine, PPh$_3$) Complexes. Syntheses of nickel alkyl complexes were developed for several reasons. The nickel alkyl complexes are intermediates in the ethylene polymerization reaction, they are precursors to neutral nickel alkyl agostic complexes and are a source of an anilinotropone nickel(II) complex with a less strongly coordinated donor ligand, 2,4-lutidine. Warren has reported the synthesis of a (*β*-diketiminate)nickel(2,4-lutidine)-(ethyl) complex **12**, which is in equilibrium with the agostic
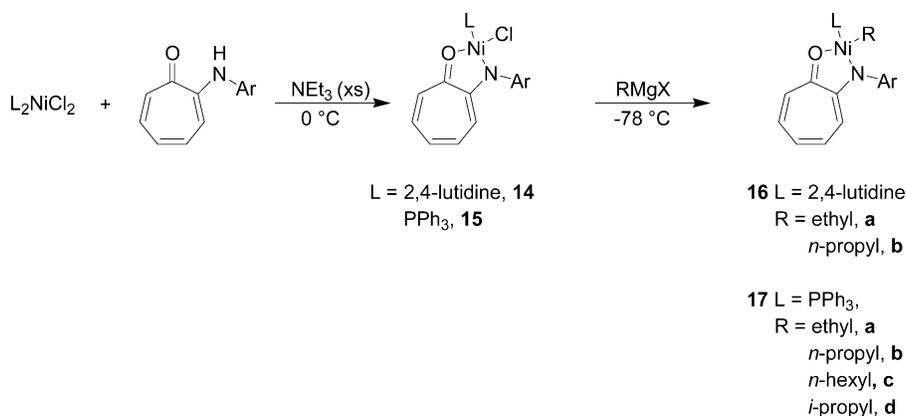
(37) Tamburlin-Thumin, I.; Crozet, M. P.; Barriere, J. C. *Synthesis* **1999**, 1149.
(38) Takeshita, H.; Mori, A. *Synthesis* **1986**, 578.
(39) Piettre, S. R. et al. *J. Med. Chem.* **1997**, *40*, 4208.
(40) Echavarren, A. M.; Stille, J. K. *J. Am. Chem. Soc.* **1988**, *110*, 1557.

Scheme 3

L$_2$NiCl$_2$ + [2-anilinotropone] →[NEt$_3$ (xs), 0 °C] [(N,O)Ni(L)(Cl) complex] →[RMgX, -78 °C] [(N,O)Ni(L)(R) complex]

L = 2,4-lutidine, **14**
PPh$_3$, **15**

16 L = 2,4-lutidine
R = ethyl, **a**
n-propyl, **b**

17 L = PPh$_3$,
R = ethyl, **a**
n-propyl, **b**
n-hexyl, **c**
i-propyl, **d**

ethyl complex, **13** (Scheme 2).[41] Upon treatment of **12** with borontrifluoride diethyl etherate, the nickel−ethyl agostic complex **13** was isolated and structurally characterized.[42,43]

Initially, an approach similar to Warren's was applied to the synthesis of an (anilinotropone)nickel(2,4-lutidine)(chloride) complex, **14**. Combination of Lu$_2$NiCl$_2$ with the sodium salt of 2-(2,6-diisopropyl)anilinotropone at a range of temperatures (−78 to 20 °C) led to the predominant formation of the bis-anilinotropone nickel complex commonly observed as the primary polymerization decomposition product (see below).[34] The lack of steric bulk of 2-anilinotropone compared to the β-diketiminate ligand likely results in the rapid reaction of 2 equiv of the sodium salt with the nickel halide. To slow the rate of reaction with the nickel center, 2-anilinotropone (rather than its sodium salt) was added to Lu$_2$NiCl$_2$ in the presence of excess triethylamine and produced **14** in high yield. Without excess triethylamine, **14** decomposes prior to workup. Complex **14** is paramagnetic and was not characterized by NMR spectroscopy. When **14** was combined with either ethylmagnesium chloride or propylmagnesium chloride in diethyl ether at −78 °C, the desired (anilinotropone)nickel(lutidine)(alkyl) complexes **16a** (ethyl) and **16b** (propyl) were formed as red powders in moderate isolated yields (55−60%, Scheme 3).

Complexes **16a,b** are both diamagnetic and were characterized by ^{1}H and ^{13}C NMR spectroscopy. The ^{1}H NMR spectrum of **16a** is representative of both complexes (See Experimental Section for complete data). Restricted rotation about the nickel−lutidine nitrogen bond renders the methine protons of the isopropyl groups inequivalent, and they appear as septets at 3.70 and 3.55 ppm. Additionally, the two methylene protons of the ethyl group are diastereotopic and appear as distinct multiplets at −0.3 and −0.5 ppm. The methyl resonance of the ethyl group appears at −0.4 ppm, between the two resonances for the diastereotopic protons.

Nickel alkyl complexes with a PPh$_3$ donor ligand were synthesized to model intermediates in the ethylene polymerization reactions. Complexes **17a−c** were obtained as orange powders in the same manner as the nickel lutidine alkyl complexes. The (anilinotropone)nickel(PPh$_3$)(isopropyl) complex, **17d**, was isolated using techniques to prevent warming above −25 °C. Filtration and workup at 20 °C led to clean

conversion to the *n*-propyl complex **17b**. The ^{1}H NMR spectrum of **17a** is representative of this class of compounds. Complex **17a** contains a plane of symmetry, and as expected, the methylene protons of the ethyl complex exhibit a single resonance at −0.5 ppm, while the methyl protons appear at −0.2 ppm. The methine protons of the isopropyl units are equivalent, exhibiting a septet resonance at 3.6 ppm. The methyl groups of the isopropyl unit are inequivalent, appearing as doublets at 1.3 and 1.0 ppm due to slow rotation about the nitrogen−aryl bond.

A nickel-hydride species has been proposed as an intermediate in the ethylene oligomerization cycle of several neutral nickel SHOP-type catalysts.[31,44] Keim has reported the synthesis of the nickel hydride complex, **19**, by reaction of Ni(COD)$_2$ with phosphino alcohol **18** and tricyclohexylphosphine in toluene at −10 °C (eq 2).[44] A similar attempt was made to synthesize (N,O)Ni(PPh$_3$)(H) (**20**) (N,O = 2,6-diisopropylanilinotropone) by reaction of the anilinotropone ligand with Ni(COD)$_2$ and either PPh$_3$ or PCy$_3$. In both cases, the only product obtained was the bis-anilinotropone nickel(II) complex (see below).

18 + Ni(COD)$_2$ + PCy$_3$ → **19** (2)
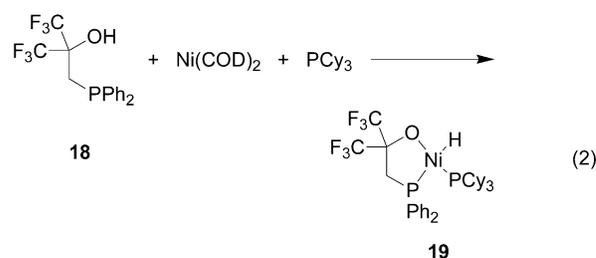
Successful synthesis of nickel hydride complex **20** was achieved using a method similar to that employed for the nickel alkyl complexes **16** and **17**. Reaction of (N,O)Ni(PPh$_3$)(Cl), **15**, with excess NaHB(OMe)$_3$ at −78 °C led to clean conversion to the desired nickel hydride (N,O)Ni(PPh$_3$)(H), **20** (eq 3). NaHB(OMe)$_3$ was chosen as the hydride source because of the known lack of reactivity of the B(OMe)$_3$ byproduct. A nickel hydride resonance was observed at −26.7 ppm with a J_{PH} coupling constant of 130 Hz, similar to the hydride resonance for **19** at −25.0 ppm.[44] The ^{31}P NMR spectrum of **20** exhibited a doublet at 31.8 ppm (J_{PH} = 123 Hz).

Chain Propagation Studies. Catalysts **9c,d** were synthesized to investigate electronic effects on ethylene polymerization. The results of ethylene polymerization with *p*-methoxyphenyl-**9c**,

(41) Wiencko, H. L.; Kogut, E.; Warren, T. H. *Inorg. Chim. Acta* **2003**, *345*, 199.
(42) Warren, T. H.; Wienko, H. L.; Kogut, E.; Dai, X.; McDermott, J. *International Symposium on Olefin Metathesis*, Cambridge, MA, 2001.
(43) Kogut, E.; Zeller, A.; Warren, T. H.; Strassner, T. Personal communication.
(44) Muller, U.; Keim, W.; Kruger, C.; Betz, P. *Angew. Chem., Int. Ed.* **1989**, *28*, 1011.

$$\delta = -26.7 \text{ ppm}$$
$$J_{PH} = 130 \text{ Hz}$$

(3)

20
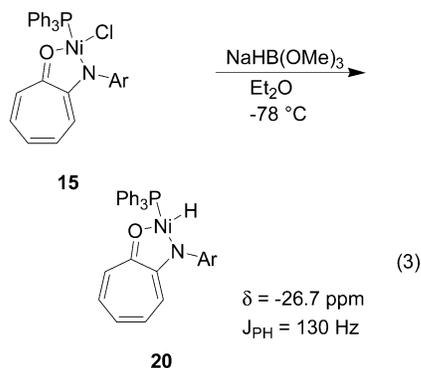
phenyl-**9a**, and *p*-trifluoromethylphenyl-**9d**-substituted catalysts are summarized in Table 1. The polymerizations were performed in a water-cooled reactor at sufficiently low catalyst loadings to avoid reaction exotherms greater than 2 °C. Therefore, reliable comparisons of catalyst activity and lifetime are possible.[45] At 40 and 60 °C, no clear trend is evident in overall catalyst turnover numbers; however, at 60 °C the *p*-methoxyphenyl-substituted catalyst **9c** is noticeably less active than **9a** or **9d** with TONs of 19 000, 32 000, and 27 000, respectively. At 80 °C, the turnover number clearly increases from 59 500 (**9c**) to 64 300 (**9a**) to 70 000 (**9d**) as the electron-withdrawing nature of the anilinotropone ligand increases. When reaction times are increased to 1 h, the trend is even more evident, with an increase in turnover number from 72 000 (**9c**) to 87 700 (**9a**) to 110 800 (**9d**). No significant differences in M_n or molecular weight distribution are observed for the three catalysts at any of the polymerization temperatures investigated. As expected,[10,12] branching increases with increasing temperature. The branching numbers for the three catalysts are relatively uniform with slightly higher values for **9a**. Molecular weight distributions of ca. 2 at 60 and 80 °C indicate that the molecular weights obtained are chain-transfer limited. At 40 °C, the MWDs of ca. 1.4 indicate that, after 10 min, the chain-transfer-limited M_n is not reached and that longer reaction times would yield higher M_n values.

The reactions of ethylene with anilinotropone nickel(II) complexes **3** and **9a** were investigated by *in situ* NMR spectroscopic studies at low temperatures. The rate of insertion of ethylene into the Ni-phenyl bonds of both unsubstituted **3** and phenyl-substituted **9a** to form, initially, the corresponding (N,O)Ni(PPh₃)CH₂CH₂Ph complexes, was determined by monitoring the decrease in concentrations of **3** and **9a**. In a typical experiment, the catalyst was dissolved in CD₂Cl₂ and then cooled to −78 °C, and ethylene was injected into the NMR sample, which was then inserted into a precooled NMR probe. The resonances associated with the methyl and methine groups of the isopropyl moiety were used to measure relative concentrations of the starting complex and single- and double-(multiple) insertion products. The first-order rate constants, as illustrated in Scheme 4, were measured as a function of temperature and ethylene concentration and are summarized in Table 2.

Even at high ethylene concentrations, only PPh₃ complexes are observed (no ethylene complexes are detected). As shown

(45) Typically, more electron-withdrawing ligands lead to higher polymerization activities for neutral nickel catalysts. See, for example: Cavell, K. *J. Organomet. Chem.* **1997**, *544*, 163. Johnson, L. K. et al. WO 98/30609, 1998.

Table 1. Ethylene Polymerization with **9a**, **9c**, and **9d**[a]

entry	catalyst	T(°C)	psig	t(min)	TON	M_n(×10⁻³)	M_w/M_n	branches/1000 C
1	**9c**	40	200	10	9100	202	1.4	16
2	**9c**	60	200	10	19 000	220	1.9	34
3	**9c**	80	200	10	59 500	100	2.1	64
4	**9a**	40	200	10	9600	251	1.3	34
5	**9a**	60	200	10	32 000	194	2.1	41
6	**9a**	80	200	10	64 300	87	2.2	76
7	**9d**	40	200	10	9400	242	1.4	15
8	**9d**	60	200	10	27 300	235	1.9	31
9	**9d**	80	200	10	70 000	102	1.8	64

[a] Reactions were run in 200 mL of toluene with 6.6 μmol of catalyst.

Scheme 4
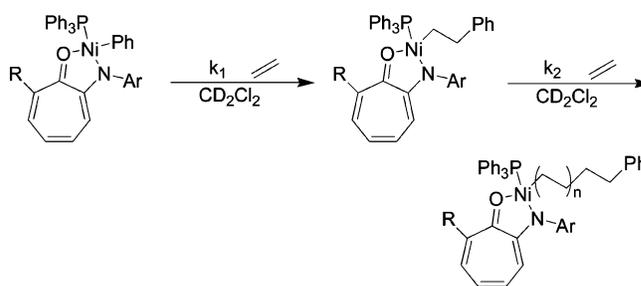
Table 2. Ethylene Insertion into the Ni−Ph Bond of Catalysts **3** and **9a** (Catalyst Concentration of 10.6 mM in CD₂Cl₂)

| entry	catalyst	T (°C)	C₂H₄ (equiv)	[C₂H₄] (mM)	$k_{1(obs)}$ (×10⁵ sec⁻¹)	k_1 (×10⁴ M⁻¹ sec⁻¹)
1	**3**	−10	16	170	2.6	1.5
2	**3**	−10	24	254	3.5	1.4
3	**3**	0	8	85	9.3	10.9
4	**3**	10	14	149	34.4 (3.4)[a]	23.2 (2.3)[a]
5	**3** + 5 equiv of PPh₃	10	12	128		
6	**9a**	−10	12	128	3.0	2.5

[a] Subsequent insertion of ethylene into the nickel−alkyl bond

in entries 1 and 2, insertion rates exhibit a first-order dependence on [C₂H₄]. As expected, rates accelerate with temperature, increasing about an order of magnitude between −10 and 10 °C (compare entries 1 and 4). Insertion is dramatically inhibited by [PPh₃], as shown in entry 5. (Under these conditions the NMR spectrum of **3** is unchanged, indicating that inhibition is not due to formation of a five-coordinate bis-phosphine species.) The first insertion of ethylene into the Ni−aryl bond of **3** is significantly faster than the second insertion into the Ni−alkyl bond of (N,O)Ni(CH₂CH₂Ph)(PPh₃), and thus this first insertion product builds up in high concentrations. Analysis of the kinetics as two consecutive first-order reactions allows estimation of k_2 (entry 4), which is an order of magnitude less than k_1. (This result implies that insertion into the Ni−phenyl bond does not constitute a slow initiation step.)

The mechanistic scenario shown in Scheme 5 involving a rapid pre-equilibrium strongly favoring the phosphine complex, followed by a slow insertion step, is clearly supported by the observation that the catalyst resting states are exclusively PPh₃ complexes and the insertion rates are first-order in [CH₂CH₂] and strongly inhibited by PPh₃. The overall rate will be controlled by both the equilibrium constant, K_{eq}, and the insertion rate constant, k_{ins}. Comparing entries 2 and 6 in Table 2 shows that the 7-phenyl-substituted system, **9a**, inserts ethylene at a rate slightly faster than that of unsubstituted **3** (i.e., correcting for [CH₂CH₂], $k_1(\mathbf{9a})/k_1(\mathbf{3}) = 1.8$.). Since k_1 is

Scheme 5
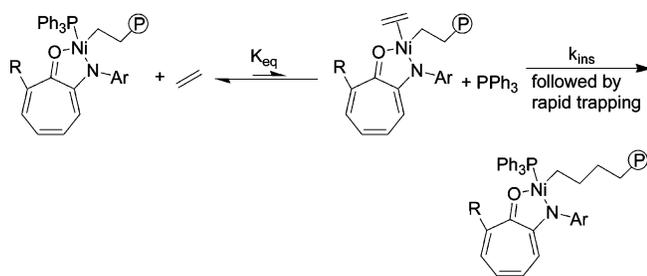
Table 3. Exchange of PPh$_3$ by P(p-Tolyl)$_3$ at −14 °C in CD$_2$Cl$_2$

entry	catalyst	[Ni] (mM)	[P(p-tolyl)$_3$] (mM)	k[PPh$_3$] (s^{-1})	k (M^{-1} s^{-1})
1	**3**	10.6	117	6.4×10^{-4}	5.5×10^{-3}
2	**3**	10.6	318	25×10^{-4}	7.9×10^{-3}
3	**9a**	9.4	141	9.3×10^{-4}	6.6×10^{-3}
4	**9a**	9.4	273	18.6×10^{-4}	6.8×10^{-3}

proportional to $K_{eq}k_{ins}$, the effect of aryl substitution on the individual values of K_{eq} and k_{ins} cannot be determined from these data.

Scheme 5 requires exchange of ethylene for PPh$_3$, and since the ethylene complex cannot be observed, the nature of the exchange, associative or dissociative, cannot be determined. To model this process we examined displacement of PPh$_3$ by P(p-tol)$_3$. Use of high concentrations of P(p-tol)$_3$ shifts the equilibrium shown in eq 4 sufficiently far to the right that simple first-order kinetics are observed.
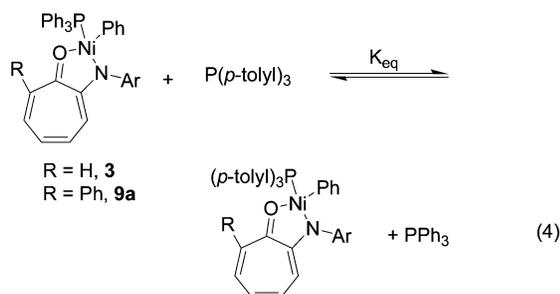

R = H, **3**
R = Ph, **9a**

$$\text{(4)}$$

Table 3 summarizes data for **3** and **9a** at −14 °C. Rates are first order in P(p-tol)$_3$, and displacement is clearly associative. These results are consistent with the expected mechanism of ligand exchange at a 16-electron d^8 square planar metal center and suggest that ethylene exchanges with triphenylphospine by an analogous associative mechanism. The addition of the sterically bulky phenyl group in the 7-position of **9a** has little effect on the rate of phosphine exchange.

Several preparative-scale polymerization reactions were carried out that support and amplify the mechanism suggested by the NMR spectroscopic studies.

We first examined the effects of added triphenylphosphine on ethylene polymerization. Standard conditions were employed (200 psig CH$_2$CH$_2$, 7.4 μmol of catalyst, 200 mL of toluene) in the presence of a specified amount of PPh$_3$. Exotherms were less than 2 °C. Reactions were performed with both the unsubstituted catalyst **3** and the naphthyl-substituted catalyst **9b** at 80 and 40°C, respectively. The results are summarized in Table 4.

The addition of 5 equiv of added triphenylphosphine to catalyst **3** at 80 °C and 200 psig ethylene has little effect on the

Table 4. Ethylene Polymerization with **3** and **9b** in the Presence of PPh$_3$ in 200 mL of Toluene and 7.4 μmol of Catalyst at 200 psig Ethylene

entry	catalyst	T (°C)	t (min)	TON	M_n ($\times 10^{-3}$)	M_w/M_n	branches
1	**3**	80	10	51 500	92	1.8	72
2	**3** + 5 equiv of PPh$_3$	80	10	43 400	54	2.3	68
3	**3**	80	30	60 400			
4	**3** + 5 equiv of PPh$_3$	80	30	60 000	67	2.3	67
5	**3** + 50 equiv of PPh$_3$	80	15	5600	33	1.9	60
6	**3** + 50 equiv of PPh$_3$	80	60	16 400	31	2.1	58
7	**3** + 50 equiv of PPh$_3$	80	180	18 100	33	2.0	57
8	**9b**	40	10	11200	250	1.3	22
9	**9b**	40	60	50 600	831	3.8	9
10	**9b** + 5 equiv of PPh$_3$	40	10	2700	77	1.4	13
11	**9b** + 5 equiv of PPh$_3$	40	60	13 300	382	1.9	9

polymerization.[46] After 10 min, the turnover number (TON) is slightly reduced (compare entries 1 and 2); however, after 30 min, the turnover numbers are essentially identical (entries 3 and 4). Under these conditions of high temperature and high ethylene concentration, the equilibrium (Scheme 5) must very substantially favor the ethylene complex and be only slightly shifted to the left by addition of 5 equiv of PPh$_3$. At 50 equiv, a substantial effect on the equilibrium is observed (entries 5−7). For example, TONs drop from 51 500 in 10 min with no added PPh$_3$ to 5600 in 15 min with 50 equiv of added PPh$_3$. These results also suggest that the addition of PPh$_3$ increases the lifetime of **3**. Typically, in the absence of PPh$_3$ at 80 °C and 200 psig ethylene, TONs increase only slightly when reaction times are increased from 10 to 60 min (52 400 to 62 100).[36] However, with 50 equiv of added PPh$_3$, the TON at 60 min (16 400) increases 3-fold relative to the TON at 15 min. Further polymerization (3 h) leads to only slightly increased TONs (entry 7). (Further discussion of catalyst lifetimes appears below.)

The effect of excess PPh$_3$ at lower temperatures was investigated with 7-naphthyl-substituted catalyst **9b**. Due to the long lifetime of **9b** at 40 °C,[36] the only effect of added PPh$_3$ will be an effect on the equilibrium between Ni−PPh$_3$ and Ni−ethylene complexes and not on catalyst lifetime as with **3**. In contrast to the 80 °C polymerizations, at 40 °C, 5 equiv of added PPh$_3$ has a noticeable effect on activity. After a 60 min run with no PPh$_3$ added, the overall turnover number for **9b** is 50 600 (entry 9). When 5 equiv of PPh$_3$ are added, the turnover number drops to 13 300 (entry 11). A similar drop in TON is observed for the 10 min polymerization runs (entries 8 and 10). These data suggest that at 40 °C, in the presence of 5 equiv of PPh$_3$, the equilibrium lies substantially in favor of the Ni−PPh$_3$ complex.

In addition to the activity and lifetime effects of added PPh$_3$, an influence on polymer molecular weight is also observed. With excess PPh$_3$, the number average molecular weight drops from 91.5K (no PPh$_3$, entry 1) to 53.9K (5 equiv of PPh$_3$, entry 2) to 33.1K (50 equiv PPh$_3$, entry 5). The decrease in polymer molecular weight is due to a decrease in the rate of chain propagation, while the rate of chain transfer remains approximately constant (this will be explained in more detail below). In all cases, added PPh$_3$ has little effect on the molecular weight distribution of the polymers, with all values equal to ca. 2.0. The very high molecular weight for entry 9 ($M_n = 831$K)

(46) Only 3−4 equiv of PPh$_3$ is reported to completely shut down the salicylaldimine catalysts **2a,b**. See: Younkin, T. R.; Connor, E. F.; Henderson, J. I.; Friedrich, S. K.; Grubbs, R. H.; Bansleben, D. A. *Science* **2000**, *287*, 460.

Table 5. Polymerization of Ethylene with **9a**, **16a**, **9d**, and **9b** at Catalyst Loadings of 6.6, 7.5, 6.1, 6.6 μmol, Respectively, in 200 mL of Toluene

entry	catalyst	T (°C)	psig	t (min)	TON	M_n ($\times 10^{-3}$)	M_w/M_n	branches
1	**9a**	40	50	20	5500	134	1.4	34
2	**9a**	40	100	20	10 300	280	1.6	27
3	**9a**	40	200	20	16 300	356	1.6	11
4	**9a**	40	400	20	20 500	394	1.6	10
5	**9a**	40	600	20	23 600	424	1.5	8
6	**9a**	40	800	20	22 900	431	1.6	7
7	**9a**	60	600	10	54 400			24
8	**16a**	60	100	15	16 200	82	3.1	61
9	**16a**	60	200	15	35 000	159	2.3	47
10	**16a**	60	400	15	37 800	211	2.2	33
11	**16a**	60	600	15	43 500	265	2.1	30
12	**16a**	60	600	20	55 700	245	2.2	
13	**16a**	60	800	15	41 700	305	1.9	24
14	**9c**	40	600	20	9250	376	1.5	10
15	**9d**	40	600	20	18 900	524	1.5	8
16	**9d**	40	800	20	16 900	531	1.5	7
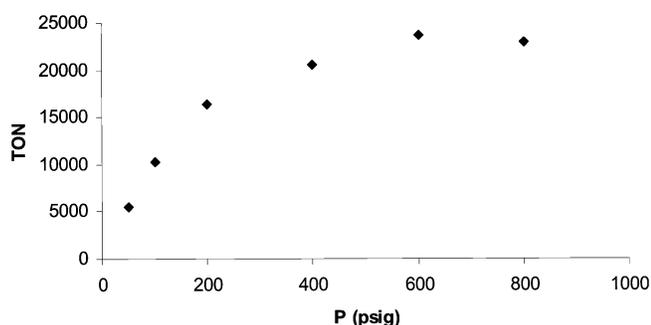
Figure 1. TON vs $P(C_2H_4)$ using catalyst **9a** at 40 °C.

leads to a viscous GPC sample, which is likely the cause of the broad molecular weight distribution observed. The polymer branching data suggest that polymerization temperature and ethylene pressure, not PPh$_3$ concentration, control the amount of branching. Similar branching numbers are observed with and without added PPh$_3$.

The proposed mechanism predicts that at sufficiently high ethylene pressures, the dominant resting state should be the nickel ethylene complex. Under these conditions the rate of chain growth will be independent of ethylene concentration and simply equal to the rate of migratory insertion. This saturation rate behavior was examined for several complexes, and data are summarized in Table 5. Phenyl-substituted catalyst **9a**, has a long lifetime at 40 °C with only a slight drop in turnover frequency from 10 to 60 min. Thus, polymerizations carried out for 20 min at 40 °C with **9a** should provide reliable values of TOFs. The activity of **9a** was screened at 40 °C (20 min runs) from 50 to 800 psig ethylene. Increasing the ethylene pressure causes an increase in polymer molecular weight from 133.9K (50 psig, entry 1, Table 5) to 431.1K (800 psig, entry 6, Table 5) and a decrease in the total number of branches per 1000 carbon atoms (34, 11, and 7 at 50, 200, and 800 psig, respectively), consistent with earlier observations. As expected for saturation behavior, the catalyst turnover number increases with pressure and gradually levels off between 600 and 800 psig ethylene. A plot illustrating this behavior is shown in Figure 1. At saturation, a turnover number of 23 600 in 20 min (600 psig, entry 5) implies a k_{ins} value of 19 s^{-1} corresponding to a free energy of activation of 16.1 kcal/mol. At 60 °C, the rate
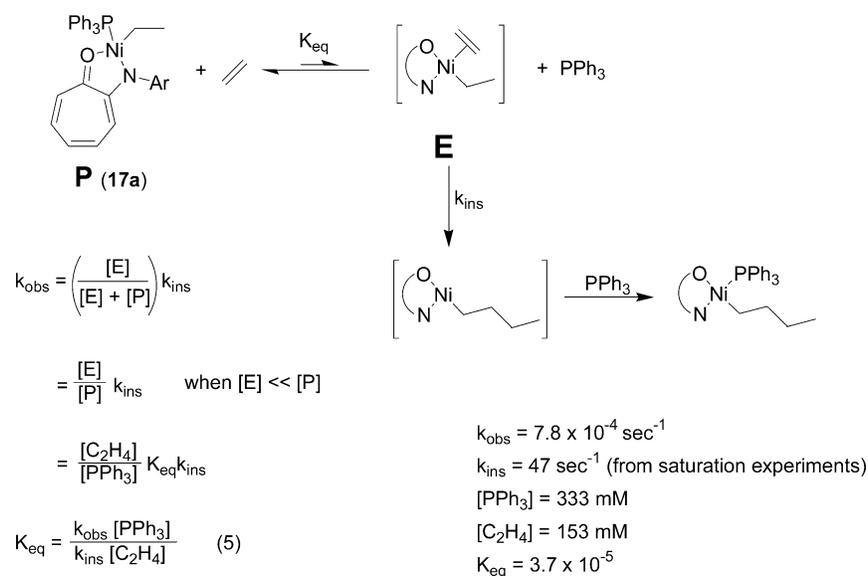
constants for insertion and $\Delta G^\ddagger$ were determined to be 91 s^{-1} and 16.6 kcal/mol, respectively (entry 7). Similar studies led to insertion barriers of 16.6 kcal/mol for the *p*-trifluoromethylphenyl-substituted catalyst **9d** (entries 15 and 16) and 17.1 kcal/mol for the *p*-methoxyphenyl-substituted catalyst **9c** (entry 14).

To determine the ethylene insertion barrier for the unsubstituted version of the anilinotropone catalyst, the 2,4-lutidine complex, (2-anilnotropone)Ni(Lu)(Et), **16a**, was employed. Initial attempts to reach saturation with the parent PPh$_3$-substituted catalyst **3** were unsuccessful. At 60 °C, where catalyst lifetime is sufficient for accurate activity determination, saturation could not be achieved at reasonable pressures (<1000 psig). At 80 °C, the lifetime of **3** is insufficient for accurate determination of catalyst activity. Therefore, a catalyst with the less strongly coordinating 2,4-lutidine donor ligand was investigated at 60 °C. A similar increase in M_n and decrease in polymer branching number (Table 5, entries 8−13) with ethylene pressure are observed. Saturation behavior is again observed with increasing ethylene pressure, and similar turnover numbers at 600 and 800 psig show that saturation has been reached. Turnover numbers of 43 500 and 55 700 for 15 and 20 min polymerizations (entries 11, 12) show that no significant catalyst decomposition occurs in the first 20 min of reaction at 60 °C. These data lead to values for k_{ins} of 48 s^{-1} and for $\Delta G^\ddagger$ of 17.0 kcal/mol.
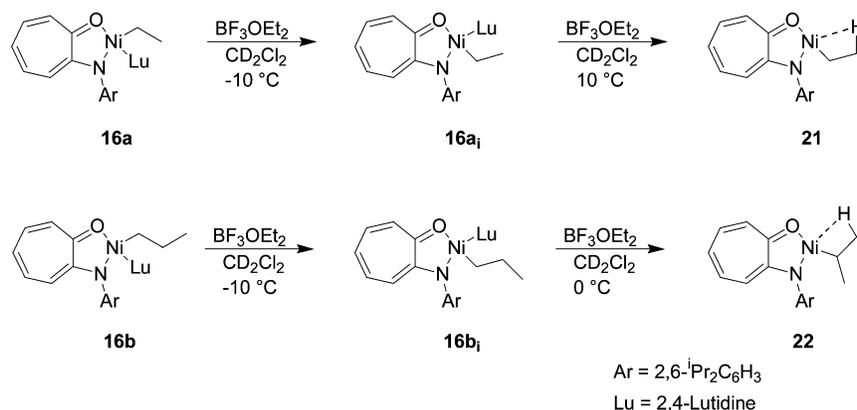
The small differences in the insertion barriers for the substituted and unsubstituted catalysts should not be over-interpreted. Errors in catalyst sample preparation, polymer collection, and polymerization temperature control could lead to errors in $\Delta G^\ddagger$ of up to 0.5 kcal/mol. With that caveat in mind, the insertion barriers range from 16 to 17 kcal/mol, with no significant difference between the aryl-substituted and unsubstituted catalysts. These values are intermediate between the values for the cationic diimine nickel catalysts (13.5−14.0 kcal/mol)[21,24] and the cationic diimine palladium catalysts (18.0−18.5 kcal/mol).[23]

In addition to determination of the value for k_{ins}, the equilibrium constant, K_{eq} (Scheme 6), between the nickel−PPh$_3$ and nickel−ethylene complexes can be estimated. K_{eq} can be calculated from k_{ins}, k_{obs}, [PPh$_3$], and [CH$_2$CH$_2$]. The observed rate constant is equal to the fraction of Ni complex, which sits as the ethylene complex ([E]/[E] + [P]) times k_{ins}. At high [PPh$_3$], the concentration of [E] will be much less than [P], and the expression simplifies to $k_{obs} = k_{ins}$[E]/[P] as shown in Scheme 6. Further manipulation yields eq 5 for K_{eq}. Since a Ni−alkyl complex is a better model for the growing polymer chain than a Ni−aryl complex, kinetics were carried out with **17a** in a manner similar to the runs described earlier in Table 2. Excess [PPh$_3$] and [CH$_2$CH$_2$] were added to the solution of **17a**, and NMR spectroscopy established [P] $\gg$ [E] (no ethylene complex detected). Kinetic measurements of insertion rates were made at 60 °C to match the temperature at which k_{ins} was measured in the saturation experiments. (Details of kinetic runs are summarized in the Experimental Section.) At 60 °C, when [PPh$_3$] = 334 M and [CH$_2$CH$_2$] = 153 M, $k_{obs} = 7.8 \times 10^{-4}$ sec^{-1}. Using the value of $k_{ins} = 47$ s^{-1} from the saturation experiments, K_{eq} can be estimated as 3.7×10^{-5}, $\Delta G° = 6.8$ kcal/mol.[47] Arguments based on model systems that suggest this K_{eq} value is in the expected range are presented in Supporting Information.

Scheme 6

$$k_{obs} = \left(\frac{[E]}{[E] + [P]}\right) k_{ins}$$

$$= \frac{[E]}{[P]} k_{ins} \qquad \text{when } [E] \ll [P]$$

$$= \frac{[C_2H_4]}{[PPh_3]} K_{eq} k_{ins}$$

$$K_{eq} = \frac{k_{obs} [PPh_3]}{k_{ins} [C_2H_4]} \qquad (5)$$

$k_{obs} = 7.8 \times 10^{-4} \text{ sec}^{-1}$

$k_{ins} = 47 \text{ sec}^{-1}$ (from saturation experiments)

$[PPh_3] = 333$ mM

$[C_2H_4] = 153$ mM

$K_{eq} = 3.7 \times 10^{-5}$

Scheme 7

Ar = 2,6-^{i}Pr$_2$C$_6$H$_3$

Lu = 2,4-Lutidine

Agostic Complex Formation and Dynamics. Agostic alkyl nickel complexes are key intermediates whose behavior controls branching in the α-diimine nickel and palladium catalysts.[10,12,23,24] Similar agostic alkyl complexes are also likely key intermediates for the introduction of branches into the polymers produced with the anilinotropone neutral nickel catalysts. To observe such intermediates, we have adopted a method similar to one developed by Warren,[41−43] wherein 2,4-lutidine can be extracted from neutral nickel alkyl complexes using boron trifluoride diethyl etherate to yield agostic alkyl species. Results are summarized in Scheme 7.

The nickel ethyl complex (N,O)Ni(Lu)(Et), **16a**, was treated with a 5−10-fold excess of BF$_3$OEt$_2$ at −78 °C in CD$_2$Cl$_2$. Upon warming, two separate processes occur. At −10 °C, **16a** converts to an isomer **16a$_i$**. Structures of **16a** and **16a$_i$** are assigned as shown in Scheme 7 on the expected greater thermodynamic stability of **16a$_i$**; we have no additional evidence for assignments. The ethyl resonances of **16a** shift from bands at −0.3 ppm (one diastereotopic methylene proton), −0.4 ppm (methyl group), and −0.5 ppm (one diastereotopic methylene proton) to bands at 0.25 ppm (one diastereotopic methylene proton), −0.15 ppm

(one diastereotopic methylene proton), and −0.7 ppm (methyl group). The isomerization is catalyzed by BF$_3$; however, the precise mechanism by which this occurs is unclear. Upon further warming to 10 °C, 2,4-lutidine is abstracted by BF$_3$ to yield an equilibrium mixture of the ethyl agostic complex, **21**, and **16a$_i$**. Decomposition was observed at temperatures above 10 °C. The temperature-dependent ^{1}H NMR spectrum of **21** indicates a highly dynamic system. At −20 °C, a broad band at −4.8 ppm that integrates to three protons is observed. This resonance is a result of rapid rotation about the C−C bond of the ethyl group, which results in site exchange between the agostic hydrogen and the two β hydrogens. Upon further cooling to −90 °C, rotation about the C−C bond is slowed and the agostic proton is observable as a triplet at −13.3 ppm with a geminal coupling constant of 16 Hz. Attempted isolation of **21** was unsuccessful.

The nickel *n*-propyl complex (N,O)Ni(Lu)(Pr), **16b**, when treated with a 5−10-fold excess of BF$_3$OEt$_2$ in CD$_2$Cl$_2$ at −10 °C, isomerizes in a manner similar to that of **16a** to yield **16b$_i$**. Complex **16b$_i$** is completely converted to the isopropyl agostic complex **22** upon warming to 0 °C; no **16b$_i$** remains. The intermediate *n*-propyl agostic complex could not be detected; its isomerization is fast relative to lutidine abstraction by BF$_3$. Complex **22** is more stable than its nickel ethyl counterpart, and no decomposition is observed at temperatures as high as

(47) This analysis assumes that the equilibrium shown in Scheme 6 is fast relative to insertion. This is supported by the fact that the first insertion is strongly inhibited by added PPh$_3$ (e.g., see entry 5, Table 2, and kinetics in Supporting Information).

Scheme 8
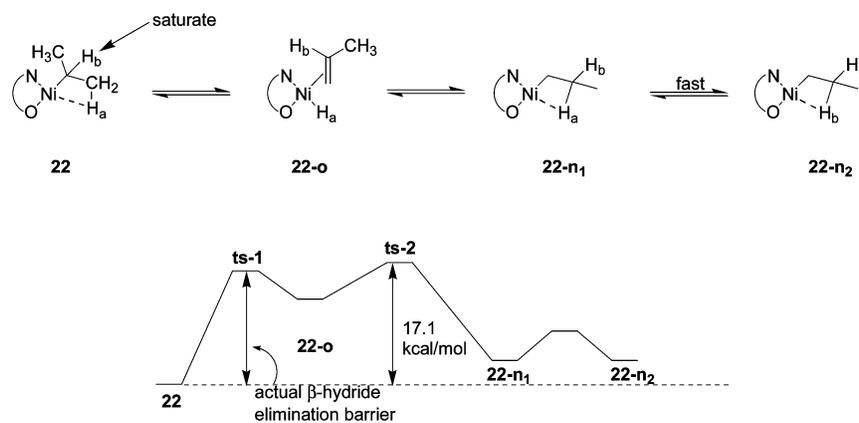
35 °C. (A similar trend in stability has been observed with the cationic α-diimine nickel agostic complexes.[24]) Complex **22** exhibits dynamic behavior. At 20 °C, the six protons of the isopropyl agostic moiety are equivalent due to rapid rotation about the nickel–methine carbon bond and are observed as a broad singlet at −2.4 ppm. Upon cooling to −40 °C, rotation about the nickel–carbon bond is slowed and two broad resonances at −0.6 and −4.3 ppm (equidistant from the −2.4 ppm midpoint), corresponding to the now inequivalent methyl groups, are observed. Upon further cooling to −90 °C a broad resonance for the agostic hydrogen is observed at −13.9 ppm.

The isopropyl agostic complex was used to quantitatively assess the dynamics of nickel–carbon bond rotation and β-hydride elimination. At the coalescence temperature (−10 °C) of the two resonances attributed to the inequivalent methyl groups, the rate of site exchange was calculated to be 3300 s^{-1}, which corresponds to a barrier to nickel–carbon bond rotation of 11.1 kcal/mol (eq 6). Spin saturation transfer techniques were used to determine an upper limit for the barrier to β-hydride elimination. The methine proton resonance at 1.3 ppm was saturated, and a decrease in the integration of the methyl proton resonance at −2.4 ppm was observed at 20 °C (Scheme 8). Quantitative analysis (see Experimental Section) leads to a rate constant for site exchange of H$_b$ to H$_a$ of 1.1 s^{-1}, $\Delta G^{\ddagger} = 17.1$ kcal/mol. This value represents an upper limit for the barrier to β-hydride elimination as shown in the free energy diagram in Scheme 8. Because the isopropyl agostic complex is more stable than the *n*-propyl agostic complex, the highest energy transition state rate in the exchange of H$_a$ and H$_b$ is likely transition state 2, which lies between the propene hydride complex, **22-o**, and the *n*-propyl agostic complex. The olefin hydride complex is expected to lie very close to the transition state;[48] thus, the 17.1 kcal/mol barrier is expected to be only slightly greater than the free energy difference between **22** and **ts-1**. By comparison, the nickel–carbon rotation and β-hydride elimination barriers for the cationic α-diimine nickel catalyst were reported to be 9.0 and 14.0 kcal/mol, respectively.[24] The β-elimination barrier in **13** is reported to be 15.1 kcal/mol.[43]
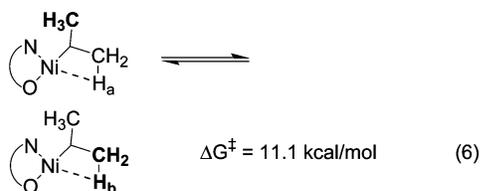
Catalyst Decomposition Studies. The products of catalyst decomposition were isolated from polymerizations carried out with the unsubstituted anilinotropone catalyst, **3**, the 7-phenyl-substituted anilinotropone catalyst, **9a**, and the previously reported 2-anilinoperinaphthenone catalyst, **4**.[35] For each polymerization (200 psig, 80 °C), the polymer was precipitated in methanol and collected by filtration. The filtrate was concentrated and analyzed for the catalyst decomposition products. From the polymerization employing the unsusbtituted anilinotropone catalyst, only the bis-anilinotropone nickel(II) complex, **25**, was isolated. The identity of the bis-ligand complex was confirmed by previously reported independent synthesis. A single-crystal X-ray structural analysis confirmed the geometry about the nickel center with the sterically bulky nitrogen atoms trans to each other.[36] Similar behavior has been reported for SHOP-type catalysts[9,49] and the salicylaldimine-based catalysts (**2a,b**).[31] From the polymerization reaction employing the 7-phenyl-substituted catalyst **9a**, the bis-anilinotropone nickel(II) complex **26** and free ligand, 2-anilino-7-phenyltropone, **8a**, were isolated. Finally the anilinoperinaphthenone catalyst decomposes exclusively to the free ligand, 2-anilinoperinaphthenone, **24**. The catalyst decomposition route for all three catalysts is likely similar, with the individual decomposition products coming at different points along the decomposition route (see below).

Treatment of the complexes **3**, **9a**, and **4** with the free ligands results in formation of benzene and the bis-ligand complexes. An NMR study was used to qualitatively estimate the rates of these reactions (Table 6). For each experiment, an NMR tube was charged with the nickel complex and its corresponding ligand in equimolar ratios. In each case, formation of the bis-ligand complex was observed via ^{1}H NMR spectroscopy at 75 °C (eq 7). Approximate half-lives are noted in Table 6. The catalyst/ligand combinations that react the fastest coincide with the catalysts that decompose to yield the highest ratios of bis-ligand complex to free ligand during polymerization. As shown in Table 6, the unsubstituted anilinotropone catalyst **3** and ligand **23** react significantly faster than the anilinoperinaphthenone catalyst **4** and ligand **24** ($t_{1/2} = <1$ and 26 h, respectively).

The rate of bis-ligand complex formation is governed by a combination of steric and electronic effects. The steric bulk of the 7-phenyl-substituted catalyst **9a** and ligand **8a** slows the

$$\Delta G^{\ddagger} = 11.1 \text{ kcal/mol} \qquad (6)$$

(48) Michalak, A.; Ziegler, T. *Organometallics* **2003**, *22*, 2069.
(49) Klabunde, U.; Tulip, T. H.; Roe, D. C.; Ittel, S. D. *J. Organomet. Chem.* **1987**, *334*, 141.

Table 6. Bis-ligand Formation Half-Lives for Catalysts **3**, **4**, and **9a** and Ligands **23**, **24**, and **8a** in C_6D_6 at 75 °C
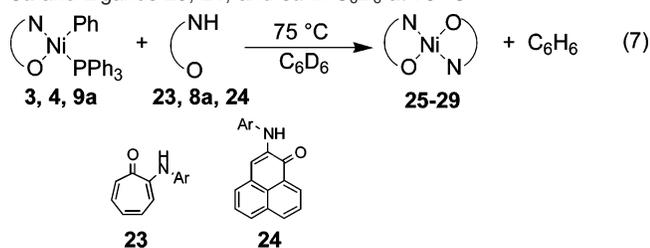
entry	catalyst (concn, mM)	ligand (concn, mM)	product	$t_{1/2}$
1	**3** (10.6)	**23** (10.6)	**25**	<1 h
2	**9a** (9.4)	**8a** (9.4)	**26**	7–8 h
3	**4** (10.6)	**24** (10.6)	**27**	26 h
4	**3** (9.4)	**24** (9.4)	**28**	>24 h
5	**4** (9.4)	**23** (9.4)	**28**	<1 h

rate of the bimolecular reaction relative to the unsubstituted catalyst **3** and ligand **23** ($t_{1/2}$ = 7–8 h and <1 h, respectively). The N–H proton of the anilinotropone ligand **23** (entry 3, Table 6) is significantly more acidic than the N–H proton of the anilinoperinaphthenone ligand **24**.[35] Therefore, the protonation of the phenyl group to give benzene, PPh₃, and bis-ligand complex is much slower for anilnoperinaphthenone than anilinotropone (entries 1 and 3). To verify that the acidity of the ligand is a determining factor in the rate of bis-ligand complex formation, a set of crossover experiments was conducted. Anilinoperinaphthenone ligand **24** and anilinotropone catalyst **3** were combined, and the rate of reaction was compared to the rate of reaction of anilinotropone ligand **23** with anilinoperinaphthenone catalyst **4** (entries 4 and 5). As expected, the more acidic anilinotropone ligand reacted significantly faster than the anilinoperinaphthenone ligand ($t_{1/2}$ < 1 h and > 24 h, respectively), supporting the contention that the acidity of the N–H proton is a determining factor in the rate of bis-ligand complex formation.

A decomposition mechanism that accounts for the range of decomposition products involves the formation of a nickel hydride complex as an intermediate in the catalytic cycle. The hydride complex can either insert ethylene and reenter the propagation cycle or reductively eliminate free ligand, thus leading to catalyst deactivation (Scheme 9). The distribution of decomposition products is then determined by the relative rate of formation of free ligand versus its rate of reaction with the nickel complex(es) present as part of the propagation cycle. In the case of anilinoperinaphthenone catalyst, **4**, the anilinoperi-naphthenone ligand **24** reacts so slowly with the propagating species that catalyst decomposition results only in formation of free ligand. For anilinotropone catalyst **3**, just the opposite it the case. Free ligand reacts rapidly with the propagating species, and only bis-ligand complex is observed. The 7-phenyl-substituted catalyst is intermediate between the two extreme cases of **4** and **3**; thus, both free ligand and bis-ligand complex are obtained.

To further probe the catalyst deactivation mechanism, the thermal stabilities of the parent anilinotropone catalyst **3** and the nickel–hexyl complex (N,O)Ni(PPh₃)(hexyl), **17c**, were investigated. (N,O)Ni(PPh₃)(Ph), **3**, is stable for hours upon heating to temperatures above 60 °C in C_6D_6. Therefore, it is unlikely that decomposition of the catalyst precursor occurs prior to initiation. However, upon heating to 50 °C in C_6D_6, hexyl

complex, **17c**, is converted to a nickel hydride complex and hexenes (ca. 90% 1-hexene, Scheme 10). The nickel hydride complex **20** that is formed is identical to independently synthesized **20** (see above). Further heating leads to the conversion of the nickel hydride to the bis-anilinotropone nickel complex. No free ligand is observed by ¹H NMR due to the rapid reaction of the aniliotropone ligand with the nickel–hexyl or nickel–hydride complex. The rate constants for the conversion of **17c** to **20** (k_1) and **20** to **25** (k_2) at 50 °C are 3.2×10^{-4} and 4.2×10^{-6} sec⁻¹, respectively.

The kinetics of the conversion to both nickel hydride and bis-ligand complex were also monitored in the presence of added PPh₃. Added PPh₃ slightly inhibits the rate of formation of the nickel–hydride complex and significantly inhibits the rate of formation of the bis-ligand complex. Table 7 summarizes the quantitative rate data for the conversion of the nickel–hexyl complex **17c** to the nickel–hydride complex **20** in the presence of various concentrations of PPh₃. A plot of k_{obs} vs 1/[PPh₃] is shown in Figure 3. The plot is linear with an intercept of 1.6×10^{-4} sec⁻¹. These data establish two routes for β-elimination, a simple first-order decay independent of PPh₃ and a second route inhibited by PPh₃. A plausible mechanism is shown in Scheme 11, and from Figure 2 and eq 9, k_1 is calculated as 1.63×10^{-4} sec⁻¹. A reasonable assumption is that the simple first-order process occurs through a five-coordinate olefin hydride intermediate.[50] The observation that the major pathway for β-elimination is a first-order process also explains the drop in molecular weight with the increase in PPh₃ concentration. With an increase in PPh₃ concentration, the rate of chain propagation will be retarded, while the rate of chain transfer via β-elimination will be essentially unaffected. Thus, the R_{ct}/R_{prop} will increase and M_n values will decrease.

$$\text{rate} = k_1[\text{S}] + \frac{k_2 K_{eq}[\text{S}]}{[\text{PPh}_3]} \qquad (8)$$

$$k_{obs} = k_1 + \frac{k_2 K_{eq}}{[\text{PPh}_3]} \qquad (9)$$

The significant inhibition of bis-ligand complex formation by excess PPh₃ suggests that reductive elimination of the anilinotropone ligand from the nickel hydride complex occurs only after PPh₃ dissociates from the nickel center. This is consistent with the observation that excess triphenylphosphine in the bulk polymerization experiments increases catalyst lifetime.

Additional Comments on the Propagation Mechanism. The propagation mechanism shown in Scheme 5 is consistent with the mechanistic data presented here. The presence of an equilibrium between the Ni(alkyl)(PPh₃) complex and the Ni-(alkyl)(ethylene) complex is supported by polymerization studies that show inhibition of catalyst activity at sufficient PPh₃ concentrations. The presence of an equilibrium is also supported by the saturation kinetics observed for polymerizations using

---

(50) A four-coordinate olefin hydride intermediate formed by initial dechelation of the carbonyl group to yield a three coordinate species cannot be ruled out. However, one might expect that if a three-coordinate species is required, the pathway involving loss of PPh₃ would be far more favorable than one involving dechelation of the carbonyl group of the bidentate ligand. We have shown in earlier work that CO insertion into a Ni(II)–alkyl can occur via a five-coordinate nickel alkyl carbonyl species that has close analogy with the proposed five-coordinate olefin hydride species. See: Shultz, C. S.; DeSimone, J. M.; Brookhart, M. *J. Am. Chem. Soc.* **2001**, *123*, 9172.
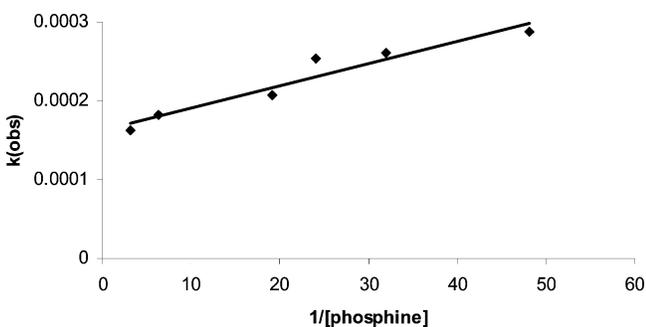
Scheme 9
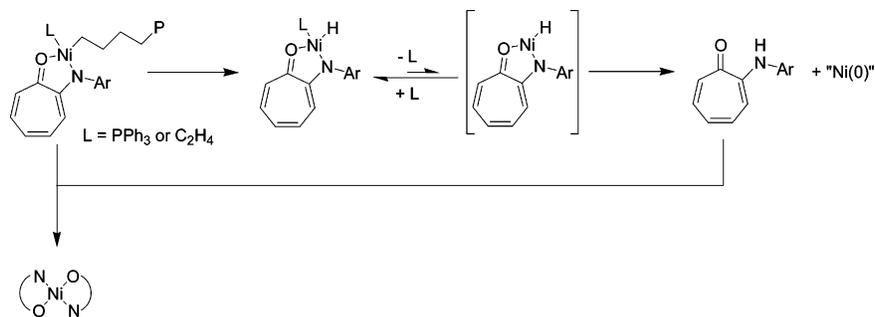
Scheme 10
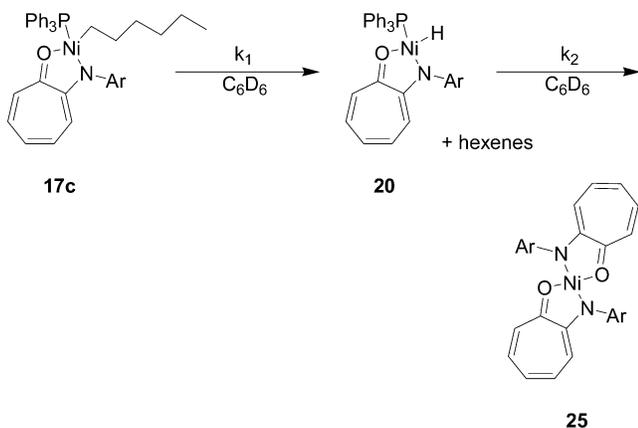
Table 7. Rate of Conversion of **17c** to **20** in the Presence of Added PPh₃ in C₆D₆ at 50 °C

entry	[PPh₃] (mM)	k_{obs} (s⁻¹)
1	20.8	2.87×10^{-4}
2	31.2	2.61×10^{-4}
3	40.6	2.54×10^{-4}
4	52.0	2.07×10^{-4}
5	156	1.82×10^{-4}
6	312	1.63×10^{-4}

Figure 2. Plot of k_{obs} vs 1/[PPh₃] for the conversion of **17c** to **20**.

9a at 40 °C as ethylene pressure is increased to 800 psig. The propagation mechanism also implies that a more weakly coordinating donor ligand should lead to a more active polymerization catalyst and saturation of the turnover frequency at lower ethylene pressures. Complex **16a**, containing the more weakly bound 2,6-lutidine ligand, is significantly more reactive than the PPh₃ analogue, **3**, at 600 and 800 psig ethylene at 60 °C (Table 8). The resting state(s) for **3** during polymerization is still an equlibrium between the two species at 600 and 800 psig (saturation has not been reached), while the lutidine
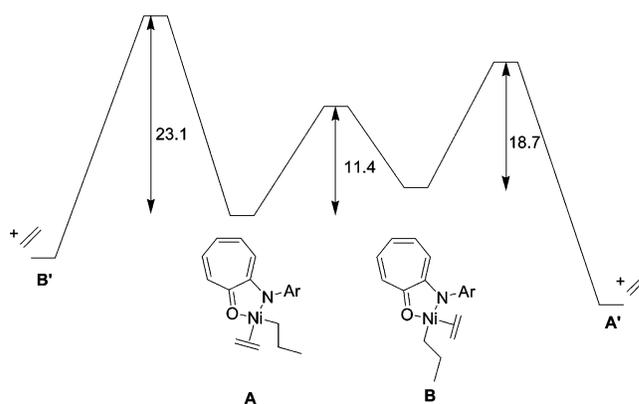

Figure 3. Ethylene insertion barriers and isomerization barriers for **A** and **B** in kcal/mol as calculated by Ziegler.

complex **16a** has reached maximum activity and "rests" as the nickel–ethylene complex at these pressures.

The nature and reason for formation of branched polyethylene formed by **3** has been discussed previously.[36] Variable-temperature and -pressure experiments with **3** suggest the mechanism depicted in Scheme 12, which mirrors the mechanism suggested for branching in the diimine catalyst system, **1**.[10,12] A branch in the polymer is introduced first by β-hydride elimination of a growing polymer chain followed by olefin rotation and reinsertion with opposite regiochemistry. This process may occur many times prior to ethylene insertion and therefore lead to methyl as well as higher branches. As ethylene pressure is increased, monomer coordination and insertion becomes more favorable and therefore the unimolecular branching pathway is less favored. Conversely, as temperature is increased, the unimolecular branching pathway is increasingly favored over ethylene coordination and insertion and therefore more branching is observed. The observation that the number of branches depends on the temperature and pressure of polymerization is consistent with the observation that the barriers to ethylene insertion and β-hydride elimination are similar (16–17 and 17.1 kcal/mol). It is of interest to note that the insertion and β-elimination barriers are similar for these neutral Ni catalysts (ca. 16–17 kcal/mol), a feature that also applies to the cationic Ni diimine catalysts (13–14 kcal/mol).[24]

Two possible isomers exist for nickel alkyl and aryl complexes. For the phosphine complexes, the more stable isomer is the one in which the alkyl/aryl group is trans to the weaker donor oxygen as expected on electronic grounds. It is reasonable to assume that this geometry, **A**, is also that of the more stable alkyl olefin complexes. However, since this isomer may readily interconvert with isomer **B**, it is unclear from which one insertion occurs. Ziegler has recently reported DFT-based

Scheme 11
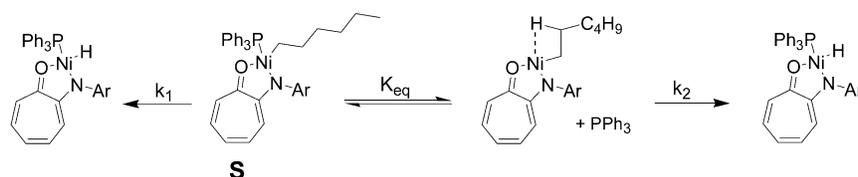
$$\text{rate} = k_1[S] + \frac{k_2 K_{eq}[S]}{[PPh_3]} \qquad (8)$$

$$k_{obs} = k_1 + \frac{k_2 K_{eq}}{[PPh_3]} \qquad (9)$$

Table 8. Ethylene Polymerization with Catalysts **3** and **16a** with a Catalyst Loading of 6.6 μmol in 200 mL of Toluene at 60 °C

entry	catalyst	P (psig)	TON
1	**3**	600	8600
2	**3**	800	17 900
3	**16a**	600	43 500
4	**16a**	800	41 700

calculations on catalyst **3** that suggest that insertion occurs from the less stable isomer **B** (ethylene trans to oxygen, Figure 3) to form **A′**, an agostic complex with the alkyl group trans to oxygen.[48] Insertion from **B** is calculated to be ca. 4.4 kcal/mol more favorable than insertion from the more stable isomer, **A**. Ziegler also estimates, on the basis of calculations on the salicylaldimine−nickel system, that the barrier to isomerization between **A** and **B** is 11.4 kcal/mol.[25]

The fact that the molecular weight significantly increases with ethylene pressure (e.g., for complex **9a** M_n = 134K, 50 psig; 280K, 100 psig; 356K, 200 psig, entries 1−3, Table 5) suggests that chain transfer to monomer is not the major chain transfer mechanism. Theoretical calculations have suggested that for similar systems, the alkyl olefin intermediate in the polymerization may partition as shown in eq 10 (Scheme 13).[26,27] Pathway a represents insertion and propagation, while pathway b represents chain transfer to monomer. If chain transfer to monomer is the sole chain transfer mechanism, then the ratio of rates of chain transfer and propagation, R_{ct}/R_p, should be independent of ethylene concentration and thus the chain transfer limited molecular weight should be independent of ethylene concentration. Since this is not observed, a chain transfer process that, at least in large part, is not dependent on ethylene concentration must occur. This is best rationalized by a conventional β-hydride elimination mechanism, shown in eq 11, that has been observed in the themolysis of the nickel hexyl complex **17c**. Of course, given the qualitative M_n values and the substantial error in these determinations, it is possible that some chain transfer occurs via the chain transfer to monomer pathway.

Summary

The studies reported here provide the first in-depth description of the mechanism of ethylene polymerization catalyzed by neutral Ni(II) complexes and allow a detailed comparison to the related cationic Ni diimine systems. Key findings are summarized below:

For the (N,O)Ni(R)(PPh$_3$) complexes, the catalyst resting state(s) are an equilibrium mixture of (N,O)Ni(R)(PPh$_3$) and (N,O)Ni(R)(C$_2$H$_4$) complexes. At high ethylene pressures, the equilibrium can be shifted strongly to the side of the ethylene complex and turnover frequency becomes independent of ethylene pressure(saturation conditions).

From mesurement of the turnover frequencies under saturation conditions, the barriers to migratory insertion in (N,O)Ni(R)-(C$_2$H$_4$) complexes were determined to lie in the range of 16−17 kcal/mol, ca. 2−3 kcal/mol greater than the barriers to insertion in cationic diimine complexes.

Intermediate (N,O)Ni(alkyl) complexes possess a β-agostic structure and exhibit dynamic behavior similar to the cationic alkyl diimine complexes. The barrier to β-elimination and readdition (chain-walking) is ca. 17 kcal/mol. Rotation around Ni−C$_\alpha$ in these complexes occurs with a barrier of 11.1 kcal/mol. These isomerization processes account for branched polyethylenes formed from these catalysts and mimic behavior previously observed with nickel and palladium diimine catalysts.
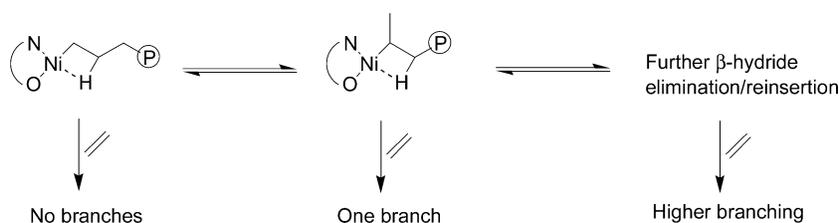
Thermolysis of the (N,O)Ni(hexyl)(PPh$_3$) complex yields the nickel hydride complex via β-elimination. Kinetic studies establish a dual pathway, a (dominant) simple first-order process and a process inhibited by PPh$_3$ involving reversible loss of phosphine. This process is a model for chain transfer and clearly explains why polymer molecular weights decrease with increasing [PPh$_3$]. The rate of propagation is retarded by increasing [PPh$_3$], while the rate of chain transfer is unchanged, resulting in an increase in R_{ct}/R_{prop}. These results argue against a chain transfer to monomer process, which would exhibit a rate inhibition equal to that for R_{prop} with added PPh$_3$

Reductive elimination of the free ligand occurs from the hydride, (N,O)Ni(H)(PPh$_3$) and is inhibited by added PPh$_3$. Such a process, combined with reaction of the free ligand with propagating nickel species, accounts for the catalyst decay process and the mixture of catalyst decay products observed, which includes the free ligands and bis-ligand complexes.
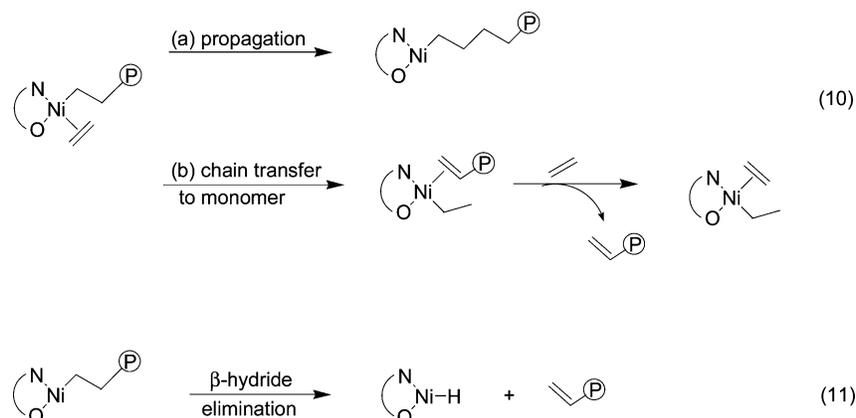
Experimental Section

General Considerations. Argon was purified by passage through columns of BASF R3-11 catalyst (Chemalog) and 4 Å molecular sieves. Toluene and pentane were deoxygenated and dried over a column of activated alumina. THF was distilled under a nitrogen atmosphere from sodium benzophenone ketyl prior to use. Triethylamine, triphenylphosphine, tri-*p*-tolylphosphine, and boron trifluoride diethyl etherate were

Scheme 12

No branches   One branch   Higher branching

Further β-hydride elimination/reinsertion

Scheme 13

(a) propagation   (10)

(b) chain transfer to monomer

β-hydride elimination   (11)

used as received from Aldrich; $(PPh_3)_2NiCl_2$ was used as received from Strem. Polymer-grade ethylene was used as received from Matheson. Some studies were conducted utilizing Research Plus-grade ethylene obtained from Matheson; the purity level is 99.9996%. Anilinotropone catalyst **3**,[34] anilinotropone **27**,[51] anilinoperinaphthenone catalyst **4**,[35] anilinoperinaphthenone **28**,[35] 2-methoxy-7-*p*-methoxyphenyltropone **5c**,[52] 2-methoxy-7-*p*-trifluoromethylphenyltropone **5d**,[52] 7-*p*-methoxyphenyltropolone **6c**,[39] 7-*p*-trifluoromethylphenyltropolone **6d**,[39] 2-triflato-7-*p*-methoxyphenyltropone **7c**,[40] 2-triflato-7-*p*-trifluoromethylphenyltropone **7d**,[40] 2-methoxytropone,[37] 2-methoxy-7-bromotropone,[38] and Lu_2NiCl_2[53] were prepared according to literature procedures.

All ^{1}H NMR chemical shifts are reported in parts per million (ppm) downfield from tetramethylsilane referenced to residual solvent ^{1}H signals. All ^{13}C NMR chemical shifts are reported in ppm relative to residual ^{13}C of the solvent. ^{31}P NMR shifts are reported relative to H_3PO_4 external standard. ^{1}H NMR spectra of polyethylenes were recorded in C_6D_5Br at 120 °C. The formula used to calculate branching was $(CH_3/3)/[(CH + CH_2 + CH_3)/2] \times 1000 =$ branches per 1000 carbons. CH_3, CH_2, and CH refer to the integration obtained for the methyl, methylene, and methine resonances, respectively. ^{13}C NMR spectra of polyethylenes were recorded in a 0.05 M $Cr(acac)_3$ solution in bromobenzene-d_5 with 15 wt % polymer. Peaks were assigned as described by Cotts.[18] High-temperature gel permeation chromatography (GPC) was performed by DuPont (Wilmington, DE) in 1,2,4-trichlorobenzene at 135 °C using a Waters HPLC 150C equipped with Shodex columns. A calibration curve was established with polystyrene standards, and universal calibration was applied using Mark–Houwink constants for polyethylene ($k = 4.34 \times 10^{-4}$; $R = 0.724$). M_n values for low-molecular weight polymer samples were determined by ^{1}H NMR end group analysis. Elemental analyses were performed by Atlantic Microlab, Inc., of Norcross, GA.

General Procedure for the Preparation of 7-Aryl-2-anilinotropones. A flame-dried Schlenk tube was charged with 7-aryl-2-triflatotropone (1.0 equiv), ground cesium carbonate (1.4 equiv), $Pd_2(dba)_3$ (2.5 mol %), and racemic BINAP (5 mol %) under an atmosphere of argon. Toluene (2 mL/mmol triflatotropone) and 2,6-

diisopropylaniline were added sequentially, and the reaction mixture was stirred at 90 °C under argon. After the specified reaction time, the reaction mixture was cooled to room temperature, diluted with CH_2Cl_2, and filtered through a pad of Celite. The solution was concentrated, and the residue was chromatographed on silica gel with 15% ethyl acetate in hexanes as the eluent.

2-(2,6-Diisopropylanilino)-7-*p*-methoxyphenyltropone, 8c. 2-Triflato-7-*p*-methoxyphenyltropone (1.40 g, 3.89 mmol) and 880 µL (4.67 mmol) of 2,6-diisopropylaniline were converted to anilinotropone **8c** in 20 h (760 mg, 50%). ^{1}H NMR (CDCl_3, 400 MHz): δ 8.7 (bs, 1H); 7.6 (m, 3H); 7.4 (m, 1H); 7.25 (m, 2H); 7.0 (m, 3H); 6.75 (t, $J = 10$ Hz, 1H); 6.3 (d, $J = 10$ Hz, 1H); 3.85 (s, 3H); 2.9 (sept, $J = 5$ Hz, 2H); 1.13 (d, $J = 3$ Hz, 6H); 1.10 (d, $J = 3$ Hz, 6H). ^{13}C NMR (CDCl_3, 100 MHz): δ 174.5, 159.4, 157.3, 147.2, 143.7, 141.2, 139.3, 135.4, 133.1, 131.4, 130.9, 129.4, 129.0, 128.8, 125.9, 124.6, 123.0, 113.9, 110.9, 55.8, 28.9, 25.0, 23.7. Anal. Calcd for $C_{26}H_{29}NO_2$: C, 80.59; H, 7.54; N, 3.61. Found: C, 80.87; H, 7.40; N, 3.30.

2-(2,6-Diisopropylanilino)-7-*p*-trifluoromethylphenyltropone, 8d. 2-Triflato-7-*p*-trifluoromethylphenyltropone (260 mg, 0.65 mmol) and 148 µL (0.78 mmol) of 2,6-diisopropylaniline were converted to anilinotropone **8d** in 20 h (130 mg, 48%). ^{1}H NMR (CDCl_3, 400 MHz): δ 8.7 (bs, 1H); 7.7 (s, 4H); 7.5 (d, $J = 7$ Hz, 1H); 7.35 (d, $J = 5$ Hz, 1H); 7.2 (d, $J = 7$ Hz, 2H); 7.0 (t, $J = 5$ Hz, 1H); 6.7 (t, $J = 5$ Hz, 1H); 6.3 (d, $J = 7$ Hz, 1H); 2.9 (sept, $J = 5$ Hz, 2H); 1.1 (d, $J = 5$ Hz, 12H). ^{19}F NMR (CDCl_3, 376 MHz): δ -62.9 (s).

Procedure for the Preparation of 2-Anilino-7-aryltroponeNi(PPh_3)(Ph) Complexes. A flame-dried Schlenk tube was charged with the appropriate anilinotropone (1.0 equiv) and sodium hydride (5.0 equiv) under an atmosphere of argon. THF (ca. 30 mL) was added, and the reaction mixture was stirred for 18 h. Then, $(PPh_3)_2Ni(Ph)Cl$ (1.0 equiv) was added as a solid, and the reaction mixture was stirred for 1 h and then filtered through a pad of Celite. The solvent was removed in vacuo, and the residue was recrystallized from toluene and pentane.

7-*p*-Methoxyphenyl-2-(2,6-diisopropyl)anilinotroponeNi(PPh_3)-Ph Complex, 9c. Anilinotropone **8c** (136 mg, 0.35 mmol) and 244 mg (0.35 mmol) of $(PPh_3)_2Ni(Ph)Cl$ were converted to the desired product (176 mg, 63%). ^{1}H NMR (CD_2Cl_2, 400 MHz): δ 7.3 (m, 9H); 7.1 (m, 7H); 6.8–7.0 (m, 5H); 6.7 (m, 3H); 6.5 (m, 1H); 6.4 (m, 3H);

(51) Hicks, F. A.; Brookhart, M. *Org. Lett.* **2000**, *2*, 219.
(52) Suri, S. C.; Nair, V *Synthesis* **1990**, *8*, 695.
(53) Machin, D. J.; Sullivan, J. F. *J. Chem. Soc. A* **1971**, *4*, 658.

6.2 (m, 1H); 6.1 (m, 2H); 3.7 (s, 3H); 3.5 (sept, $J = 5$ Hz, 2H); 1.2 (d, $J = 5$ Hz, 6H); 1.0 (d, $J = 5$ Hz, 6H). ^{13}C NMR (CD$_2$Cl$_2$, 100 MHz): δ 158.1, 144.7, 142.5, 137.7, 135.6, 134.4, 134.3, 132.8, 132.2, 132.0, 1331.7, 131.1, 129.8, 128.1, 128.0, 125.3, 123.4, 121.2, 121.1, 121.0, 113.0, 55.4, 28.8, 25.7, 23.8. ^{31}P NMR (CD$_2$Cl$_2$, 162 MHz): δ 27.0. Anal. Calcd for C$_{50}$H$_{48}$NO$_2$PNi: C, 76.54; H, 6.17; N, 1.78. Found: C, 76.56; H, 6.18; N, 1.73.

7-p-Trifluoromethylphenyl-2-(2,6-diisopropyl)anilinotroponeNi-(PPh$_3$)Ph Complex, 9d. Anilinotropone **8d** (130 mg, 0.31 mmol) and 212 mg (0.31 mmol) of (PPh$_3$)$_2$Ni(Ph)Cl were converted to the desired product (82 mg, 29%). ^{1}H NMR (CD$_2$Cl$_2$, 400 MHz): δ 7.3 (m, 10H); 7.1 (m, 10H); 6.95 (m, 3H); 6.8 (m, 1H); 6.7 (d, $J = 10$ Hz, 2H); 6.5 (m, 1H); 6.4 (d, $J = 13$ Hz, 1H); 6.2 (m, 1H); 6.1 (t, $J = 10$ Hz, 2H); 3.55 (sept, $J = 5$ Hz, 2H); 1.2 (d, $J = 5$ Hz, 6H); 1.0 (d, $J = 5$ Hz, 6H). ^{13}C NMR (CD$_2$Cl$_2$, 100 MHz) = δ 169.9, 147.1, 144.4, 142.3, 137.6, 134.3, 134.2, 132.7, 131.9, 131.4, 131.3, 130.3, 130.0, 128.2, 128.1, 125.4, 125.2, 124.4, 123.5, 121.5, 121.3, 121.1, 28.9, 25.8, 23.7. ^{31}P NMR (CD$_2$Cl$_2$, 162 MHz): δ 27.4 (s). ^{19}F NMR (CD$_2$Cl$_2$, 376 MHz): δ −63.1 (s). Anal. Calcd for C$_{50}$H$_{45}$NOPF$_3$Ni: C, 73.00; H, 5.51; N, 1.70 Found: C, 72.43; H, 5.92; N, 1.46.

2-(2,6-Diisopropyl)anilinotroponenickel(2,4-lutidine)chloride, 14. A flame-dried Schlenk tube was charged with (Lu)$_2$NiCl$_2$ (489 mg, 1.42 mmol) under argon. THF (30 mL) was added, and the mixture was cooled to 0 °C. Then, NEt$_3$ (1.0 mL, 7.2 mmol) was added followed by a THF solution (15 mL) of 2-(2,6-diisopropyl)anilinotropone. The reaction mixture was gradually warmed to room temperature over the course of 5 h and then filtered through Celite. The solvent was removed in vacuo, and the residue was recrystallized from toluene and pentane to afford paramagnetic **14** (445 mg, 65%). Anal. Calcd for C$_{36}$H$_{31}$N$_2$-ONiCl: C, 64.83; H, 6.49; N, 5.81 Found: C, 63.58; H, 6.54; N, 5.81.

2-(2,6-Diisopropyl)anilinotroponenickel(triphenylphosphine)-chloride, 15. A flame-dried Schlenk tube was charged with (PPh$_3$)$_2$-NiCl$_2$ (1.0 g, 3.55 mmol) under argon. THF (30 mL) was added, and the mixture was cooled to 0 °C. Then, NEt$_3$ (2.0 mL, 14.3 mmol) was added followed by a THF solution (15 mL) of 2-(2,6-diisopropyl)-anilinotropone. The reaction mixture was gradually warmed to room temperature over the course of 5 h and then filtered through Celite. The solvent was removed in vacuo, and the residue was recrystallized from toluene and pentane to afford paramagnetic **15** (1.98 g, 88%). Anal. Calcd for C$_{37}$H$_{37}$NPONiCl: C, 69.79; H, 5.81; N, 2.20 Found: C, 70.33; H, 5.96; N, 2.03.

2-(2,6-Diisopropyl)anilinotroponenickel(2,4-lutidine)ethyl, 16a. A flame-dried Schlenk tube was charged with (N,O)Ni(Lu)Cl, **14** (1.0 g, 2.08 mmol), under argon. Ether (30 mL) was added, and the solution was cooled to −78 °C. Ethylmagnesium chloride (2 M, 2.50 mmol) was added dropwise. Upon complete addition, the reaction mixture was stirred at −78 °C for 3 h and then warmed to room temperature and filtered through florisil. The solvent was removed in vacuo, and the product was collected (555 mg, 56%). ^{1}H NMR (CD$_2$Cl$_2$, 400 MHz): δ 9.1 (d, $J = 9$ Hz, 1H); 7.2 (s, 3H); 7.1 (s, 1H); 6.95 (m, 1H); 6.8 (t, $J = 7$ Hz, 1H); 6.6 (t, $J = 7$ Hz, 1H); 6.5 (d, $J = 9$ Hz, 1H); 6.3 (t, $J = 7$ Hz, 1H); 6.0 (d, $J = 7$ Hz, 1H); 3.7 (sept, $J = 5$ Hz, 1H); 3.55 (m, 4H); 2.3 (s, 3H); 1.4 (d, $J = 5$ Hz, 6H); 1.0 (dd, $J = 5, 5$ Hz, 6H); −0.3 (m, 1H); −0.4 (t, $J = 5$ Hz, 3H); −0.5 (m, 1H). ^{13}C NMR (CD$_2$Cl$_2$, 100 MHz): δ 179.9, 168.6, 160.4, 150.8, 148.4, 143.9, 143.0, 134.5, 132.7, 125.9, 125.6, 124.0, 122.7, 120.7, 119.9, 119.4, 28.4, 28.3, 25.9, 24.9, 23.9, 21.0, 2.4. Anal. Calcd for C$_{28}$H$_{36}$N$_2$ONi: C, 70.76; H, 7.63; N, 5.89. Anal. Calcd for C$_{28}$H$_{36}$N$_2$ONi: C, 70.76; H, 7.63; N, 5.89 Found: C, 69.10; H, 7.45; N, 5.39.

2-(2,6-Diisopropyl)anilinotroponenickel(2,4-lutidine)(n-propyl), 16b. A flame-dried Schlenk tube was charged with (N,O)Ni(Lu)Cl, **14** (1.0 g, 2.08 mmol), under argon. Ether (30 mL) was added, and the solution was cooled to −78 °C. n-Propylmagnesium chloride (2 M, 2.50 mmol) was added dropwise. Upon complete addition, the reaction mixture was stirred at −78 °C for 3 h and then warmed to room temperature and filtered through florisil. The solvent was removed in

vacuo, and the product was collected (615 mg, 61%). ^{1}H NMR (CD$_2$-Cl$_2$, 400 MHz): δ 9.1 (d, $J = 6$ Hz, 2H); 7.2 (3, 3H); 7.05 (s, 1H); 6.9 (d, $J = 6$ Hz, 1H); 6.85 (t, $J = 10$ Hz, 1H); 6.6 (t, $J = 10$ Hz, 1H); 6.5 (d, $J = 11$ Hz, 1H); 6.3 (t, $J = 9$ Hz, 1H); 6.0 (d, $J = 12$ Hz, 1H); 3.7 (sept, $J = 7$ Hz, 1H); 3.55 (m, 4H); 2.3 (s, 3H); 1.4 (vt, $J = 6$ Hz, 6H); 1.05 (dd, $J = 7, 10$ Hz, 6H); 0.4 (m, 1H); 0.3 (t, $J = 7$ Hz, 3H); 0.2 (m, 1H); −0.3 (m, 1H); −0.45 (m, 1H). ^{13}C NMR (CD$_2$Cl$_2$, 100 MHz): δ 179.9, 168.6, 160.5, 150.9, 148.3, 144.0, 142.9, 134.5, 132.6, 125.8, 125.6, 123.9, 122.7, 120.6, 120.0, 119.3, 29.1, 28.4, 26.0, 25.0, 24.2, 23.9, 23.8, 21.0, 16.4, 13.4.

2-(2,6-Diisopropyl)anilinotroponenickel(triphenylphosphine)-ethyl, 17a. A flame-dried Schlenk tube was charged with (N,O)Ni-(PPh$_3$)Cl, **15** (180 mg, 0.28 mmol), under argon. Ether (25 mL) was added, and the solution was cooled to −78 °C. Ethylmagnesium chloride (2M, 0.36 mmol) was added dropwise. Upon complete addition, the reaction mixture was stirred at −78 °C for 3 h and then warmed to room temperature and filtered through florisil. The solvent was removed in vacuo and **17a** was collected (40 mg, 22%). ^{1}H NMR (CD$_2$Cl$_2$, 400 MHz): δ 7.8 (m, 6H); 7.4 (m, 9H); 7.2 (s, 3H); 6.9 (t, $J = 7$ Hz, 1H); 6.75 t, $J = 7$ Hz, 1H); 6.5 (d, $J = 8$ Hz, 1H); 6.4 (t, $J = 7$ Hz, 1H); 6.3 (d, $J = 8$ Hz, 1H); 3.6 (sept, $J = 5$ Hz, 2H); 1.3 (d, $J = 5$ Hz, 6H); 1.0 (d, $J = 5$ Hz, 6H); −0.2 (t, $J = 5$ Hz, 3H); −0.5 (m, 2H). ^{13}C NMR (CD$_2$Cl$_2$, 100 MHz): δ 143.8, 143.3, 134.9, 134.8, 134.6, 133.5, 132.4, 132.0, 130.2, 128.9, 128.4, 128.3, 125.8, 124.2, 121.4, 120.5, 120.2, 29.0, 28.6, 24.1, 20.4, 18.5. ^{31}P NMR (CD$_2$Cl$_2$, 162 MHz): δ 34.2 (s). Anal. Calcd for C$_{39}$H$_{42}$NPONi: C, 74.07; H, 7.01; N, 2.21. Found: C, 73.78; H, 6.84; N, 2.11.

2-(2,6-Diisopropyl)anilinotroponenickel(triphenylphosphine)(n-propyl), 17b. A flame-dried Schlenk tube was charged with (N,O)-Ni(PPh$_3$)Cl, **15** (200 mg, 0.31 mmol), under argon. Ether (25 mL) was added, and the solution was cooled to −78 °C. Isopropylmagnesium chloride (2.0 M in ether, 0.38 mmol) was added dropwise, and the reaction mixture was stirred cold for 3.5 h. The reaction mixture was filtered through florisil at room temperature, during which time the product isomerized to the n-propyl isomer, and the solvent was removed in vacuo to afford 50 mg (25%) of **17b**. ^{1}H NMR (CD$_2$Cl$_2$, 400 MHz): δ 7.8 (m, 6H); 7.4 (m, 9H); 7.2 (m, 3H); 6.9 (t, $J = 10$ Hz, 1H); 6.75 (t, $J = 10$ Hz, 1H); 6.5 (d, $J = 10$ Hz, 1H); 6.4 (t, $J = 10$ Hz, 1H); 6.3 (d, $J = 11$ Hz, 1H); 3.6 (sept, $J = 7$ Hz, 2H); 1.3 (d, $J = 7$ Hz, 6H); 1.05 (d, $J = 7$ Hz, 6H); 0.5 (m, 2H); −0.2 (t, $J = 7$ Hz, 3H); −0.5 (q, $J = 8$ Hz, 2H). ^{13}C NMR (CD$_2$Cl$_2$, 100 MHz): δ 180.0, 168.9, 143.7, 143.2, 134.9, 134.6, 133.2, 132.4, 132.0, 130.2, 128.3, 125.8, 124.1, 121.4, 120.5, 28.7, 25.7, 23.8, 21.9, 16.4, 14.5. ^{31}P NMR (CD$_2$Cl$_2$, 162 MHz): δ 34.2 (s). Anal. Calcd for C$_{40}$H$_{44}$NOPNi: C, 74.55; H, 6.88; N, 2.17. Found: C, 74.15; H, 6.69; N, 1.84.

2-(2,6-Diisopropyl)anilinotroponenickel(triphenylphosphine)(n-hexyl), 17c. A flame-dried Schlenk tube was charged with (N,O)Ni-(PPh$_3$)Cl, **15** (310 mg, 0.49 mmol), under argon. Ether (25 mL) was added, and the solution was cooled to −78 °C. Hexylmagnesium bromide (2.0 M in ether, 0.62 mmol) was added dropwise, and the reaction mixture was stirred cold for 4 h. The reaction mixture was filtered through florisil at room temperature, and the solvent was removed in vacuo to afford 110 mg (33%) of **17d**. ^{1}H NMR (CD$_2$Cl$_2$, 400 MHz): δ 7.8 (m, 6H); 7.4 (m, 9H); 7.2 (m, 3H); 6.9 (t, $J = 10$ Hz, 1H); 6.75 (t, $J = 9$ Hz, 1H); 6.5 (d, $J = 10$ Hz, 1H); 6.4 (m, 1H); 6.3 (d, $J = 11$ Hz, 1H); 3.6 (sept, $J = 7$ Hz, 2H); 1.3 (d, $J = 7$ Hz, 6H); 1.0 (d, $J = 7$ Hz, 6H); 0.7 (m, 2H); 0.55 (t, $J = 7$ Hz, 3H); 0.4 (m, 4H); 0.05 (m, 2H); −0.5 (q, $J = 8$ Hz, 2H). ^{13}C NMR (CD$_2$Cl$_2$, 100 MHz): δ 180.0, 168.9, 143.6, 143.1, 135.0, 134.6, 133.2, 132.3, 131.9, 130.2, 128.4, 127.8, 124.1, 121.4, 120.4, 32.6, 31.2, 30.1, 29.1, 25.8, 24.3, 23.9, 22.8, 14.2. ^{31}P NMR (CD$_2$Cl$_2$, 162 MHz): δ 34.2 (s). Anal. Calcd for C$_{43}$H$_{50}$NOPNi: C, 75.01; H, 7.61; N, 2.04 Found: C, 73.88; H, 7.38; N, 1.96.

2-(2,6-Diisopropyl)anilinotroponenickel(triphenylphosphine)(i-propyl), 17d. A flame-dried Schlenk tube was charged with 220 mg (0.35 mmol) of (N,O)Ni(PPh$_3$)Cl, **15**, under argon. Ether (30 mL) was

added, and the solution was cooled to −78 °C. Isopropylmagnesium chloride was added dropwise, and the reaction mixture was stirred for 5 h. The reaction mixture was filtered cold through florisil, and the solvent was removed in vacuo at −30 °C to yield 80 mg (35%) of **17d**. ^{1}H NMR (CD$_2$Cl$_2$, 400 MHz): δ 7.9 (m, 6H); 7.4 (m, 9H); 7.2 (m, 3H); 6.8 (m, 2H); 6.3 (m, 1H); 6.15 (t, J = 10 Hz, 2H); 3.7 (sept, J = 7 Hz, 2H); 1.3 (d, J = 7 Hz, 6H); 1.0 (d, J = 7 Hz, 6H); 0.3 (m, 1H); −0.15 (d, J = 6 Hz, 6H). ^{13}C NMR (CD$_2$Cl$_2$, 100 MHz): δ 179.1, 168.2, 143.4, 137.2, 135.4, 134.2, 134.0, 132.8, 132.4, 130.7, 129.1, 128.5, 125.8, 123.8, 120.3, 29.0, 28.8, 25.8, 24.9, 23.9, 19.6. ^{31}P NMR (CD$_2$Cl$_2$, 162 MHz): δ 34.2 (s). The compound decomposes at temperatures above 0 °C; thus, elemental analysis was not obtained.

2-(2,6-Diisopropyl)anilinotroponenickel(triphenylphosphine)-(hydride), 20. A flame-dried Schlenk tube was charged with 400 mg (0.62 mmol) of (N,O)Ni(PPh$_3$)Cl, **15**, and 300 mg (2.35 mmol) of NaHB(OMe)$_3$ under argon. The flask was placed in an ice bath, and ether (30 mL) was added. The reaction mixture was stirred for 4 h and filtered through florisil. The solvent was removed in vacuo to afford 180 mg (48%) of the hydride product. ^{1}H NMR (C$_6$D$_6$, 400 MHz): δ 7.8 (m, 6H); 7.2 (d, J = 10 Hz, 1H); 7.1 (m, 12 H); 6.8 (t, J = 10 Hz, 1H); 6.65 (d, J = 11 Hz, 1H); 6.5 (m, 1H); 6.3 (m, 1H); 3.45 (sept, J = 7 Hz, 2H); 1.5 (d, J = 7 Hz, 6H); 1.25 (d, J = 7 Hz, 6H); −26.7 (d, J_{PH} = 130 Hz, 1H). ^{13}C NMR (C$_6$D$_6$, 100 MHz): δ 180.9, 169.3, 149.3, 141.8, 134.8, 134.5, 134.3, 133.6, 130.2, 129.0, 126.0, 124.3, 122.3, 121.8, 118.5, 28.9, 24.7, 24.2. ^{31}P NMR (C$_6$D$_6$, 162 MHz): δ 31.8 (d, J_{PH} = 123 Hz). The compound decomposes slowly at room temperature; thus, elemental analysis was not obtained.

General Procedure for High-Pressure Ethylene Polymerizations. A 1000 mL Parr autoclave was heated under vacuum up to 110 °C and then cooled to the desired reaction temperature and backfilled with ethylene. The autoclave was charged with toluene (185 mL), filled and evacuated twice with ethylene (200psig), and pressurized with ethylene to 200 psig. The stirring motor was engaged, and the reactor was allowed to equilibrate at the desired temperature for approximately 10 min. In a glovebox, a sidearm flask was charged with the catalyst. The flask was removed from the glovebox and placed on a vacuum line under Ar. The catalyst was dissolved in 15 mL of toluene and transferred via cannula into the vented autoclave with the stirring motor off. The autoclave was sealed and pressurized to the desired level, and the stirring motor was re-engaged. After the prescribed reaction time, the stirring motor was stopped, the reactor vented, and the polymer isolated via precipitation from methanol and dried in a vacuum oven. This procedure was employed with modifications in reaction time, temperature, and ethylene pressure. For studies with excess PPh$_3$, both the catalyst and PPh$_3$ were added in the same 15 mL of toluene.

General Procedure for the Reaction of (N,O)Ni(PPh$_3$)(Ph) with Ethylene. An NMR tube was charged with either catalyst **3** or **9a** and CD$_2$Cl$_2$ (700 μL) under argon and sealed with a septum. The tube was cooled to −78 °C, and ethylene was injected via syringe (2−5 mL). The sample was warmed to the desired temperature inside the NMR probe, and primary insertion was monitored by integration of resonances associates with the ligand isopropyl groups. For **3**, the original resonances were δ 3.55 (sept, 2H), 1.2 (d, 6H), and 1.0 (d, 6H). The new resonances associated with the first insertion of ethylene were δ 3.7 (sept, 2H), 1.3 (d, 6H), and 1.1 (d, 6H). Additionally, new resonances for the methylene units of the nickel−benzyl group were observed as multiplets at 1.6 and −0.3 ppm. For subsequent insertion, the methylene benzyl resonances of the singly inserted product were integrated against the new resonance of the methylene unit α to nickel at δ −0.5 ppm for the multiply inserted product. A rate of insertion was calculated by plotting the natural log of the mole fraction of starting material vs time. A representative example is shown in Supporting Information.

General Procedure for Determination of Phosphine Exchange Kinetics. An NMR tube was charged with either catalyst **3** or **9a** and

P(*p*-tolyl)$_3$ in the specified amounts under argon. The tube was sealed with a septum and cooled to −78 °C. CD$_2$Cl$_2$ (700 μL) was injected, and the tube was warmed to −14 °C in the NMR probe. Conversion was observed via ^{31}P NMR spectroscopy as the Ni−PPh$_3$ resonance at 28.6 ppm diminished as the Ni−(*p*-tolyl)$_3$ resonance at 26.3 ppm grew in. Also monitored was the appearance of free PPh$_3$ at −5.7 ppm. A pseudo-first-order rate of exchange was calculated by plotting the natural log of the concentration of starting material vs time.

General Procedure for K_{eq} Determination. An NMR tube was charged with **17a** (4 mg, 6.3 μmol), PPh$_3$ (137 mg, 523 μmol), and toluene-d_8 (700 μL) under argon and cooled to −78 °C. Ethylene was injected (4.0 mL, 115 μmol in solution), and the tube was warmed to 60 °C in the NMR probe. Insertion was monitored as with **3** and **9a**, and a pseudo-first-order rate constant was calculated by plotting the natural log of the mole fraction of **17a** vs time, yielding k_{obs} = 3.9 × 10^{-4} s^{-1}. A second experiment with **17a** (4 mg, 6.3 μmol), PPh$_3$ (61 mg, 233 μmol), and ethylene (4.0 mL, 107 μmol) gave a k_{obs} of 7.8 × 10^{-4}. K_{eq} values of 3.7 and 3.6 × 10^{-5} were calculated from each experiment.

General Procedure for the Reaction of (N,O)Ni(Lu)(R) with BF$_3$OEt$_2$. An NMR tube was charged with either **16a** or **16b** and CD$_2$-Cl$_2$ under argon. The tube was cooled to −78 °C, and 5−10 equiv of BF$_3$OEt$_2$ was injected. The tube containing **16a** and BF$_3$ was warmed to −10 °C. The following key resonances of **21** were observed: ^{1}H NMR (CD$_2$Cl$_2$, 400 MHz): δ 2.8 (bs, 3H, BF$_3$−2,4-Lutidine complex), 2.6 (bs, 3H, BF$_3$−2,4-Lutidine complex), 1.4 (m, 12H, isopropyl methyl groups), −4.8 (bs, 3H, Ni−CH$_2$CH$_3$). At −120 °C in CDCl$_2$F: δ −13.3 (t, J = 16 Hz, 1H, agostic proton).

Key resonances for **22** at 10 °C: ^{1}H NMR (CD$_2$Cl$_2$): δ 2.8 (bs, 3H, BF$_3$−2,4-Lutidine complex), 2.6 (bs, 3H, BF$_3$−2,4-Lutidine complex), 1.3 (d, J = 7 Hz, 6H), 1.0 (d, J = 7 Hz, 6H), −2.4 (bs, 6H, Ni-^{i}Pr methyls). At −40 °C: δ −0.6 (bs, 3H), −4.3 (bs, 3H). At −90 °C: δ −13.9 (bs, 1H).

Dynamics of 22, Measured Using Spin Saturation Transfer. The 1.3 ppm resonance (methine H of Ni-^{i}Pr) was saturated, and the change in the integral of the −2.4 ppm resonance (^{i}Pr methyl groups) was observed at 293K. Applying the standard equation $k = (1/T_1)[M_0/(M_{sst} − 1)]$, where M_0 = 2.77, M_{sst} = 1.76, and T_1 = 0.54 s, yields k = 1.1 s^{-1}, corresponding to $\Delta G^{\ddagger}$ = 17.1 kcal/mol (293 K).

General Procedure for Monitoring Themolysis of 17c. An NMR tube was charged with **17c**, PPh$_3$ (when appropriate), and C$_6$D$_6$ (700 μL) at room temperature under argon. The tube was warmed to 50 °C in the NMR probe, and conversion to the nickel hydride complex, **20**, followed by conversion to the bis-ligand complex, **25**, was observed by both ^{1}H and ^{31}P NMR spectroscopy. Complete conversion to **20** was observed prior to conversion of **20** to **25** A first-order rate constant for each conversion was obtained by comparing the integration of the isopropyl methine resonances at 4.0, 3.9, and 4.25 ppm for **17c**, **20**, and **25**, respectively, and plotting the natural log of the starting material mole fraction vs time. A representative plot may be found in Supporting Information.

General Procedure for Bis-Ligand Complex Formation Reactions. A J-Young tube was charged with equimolar amounts of the specified catalyst and ligand and C$_6$D$_6$ (700 μL) at room temperature. Conversion at 75 °C was observed via ^{1}H NMR spectroscopy. The concentrations for each experiment are listed in Table 6. NMR spectroscopic data for **25**[36] and **27**[35] have been previously reported.

26: ^{1}H NMR (C$_6$D$_6$, 400 MHz): δ 7.8−6.1 (m, 16H), 4.3 (sept, J = 7 Hz, 4H), 1.6 (d, J = 7 Hz, 12H), 1.4 (d, J = 7 Hz, 12 H).

28: ^{1}H NMR (C$_6$D$_6$, 400 MHz): δ 7.7−6.0 (m, 18H), 4.3 (sept, J = 7 Hz, 2H), 3.3 (sept, J = 7 Hz, 2H), 1.8 (d, J = 7 Hz 6H), 1.35 (d, J = 7 Hz 6H), 1.3 (d, J = 7 Hz, 6H), 1.15 (d, J = 7 Hz, 6H).

ship. We thank Prof. T. H. Warren for communicating unpublished results.